

A Review on Regulating Li⁺ Solvation Structures in Carbonate Electrolytes for Lithium Metal Batteries

Zhihong Piao, Runhua Gao, Yingqi Liu, Guangmin Zhou, and Hui-Ming Cheng*

Lithium metal batteries (LMBs) are considered promising candidates for next-generation battery systems due to their high energy density. However, commercialized carbonate electrolytes cannot be used in LMBs due to their poor compatibility with lithium metal anodes. While increasing cut-off voltage is an effective way to boost the energy density of LMBs, conventional ethylene carbonate-based electrolytes undergo a number of side reactions at high voltages. It is therefore critical to upgrade conventional carbonate electrolytes, the performance of which is highly influenced by the solvation structure of lithium ions (Li⁺). This review provides a comprehensive overview of the strategies to regulate the solvation structure of Li⁺ in carbonate electrolytes for LMBs by better understanding the science behind the Li⁺ solvation structure and Li⁺ behavior. Different strategies are systematically compared to help select better electrolytes for specific applications. The remaining scientific and technical problems are pointed out, and directions for future research on carbonate electrolytes for LMBs are proposed.

1. Introduction

Since the commercialization of lithium-ion batteries (LIBs) in the 1990s, the flourishing development of mobile devices and electric vehicles has led to enormous efforts in exploring high-energy-density battery systems.^[1,2] The energy density is the product of specific capacity and cut-off voltage, so increasing both is key to improving the energy density.^[3,4] However, the energy density of current commercial LIBs with a graphite (specific capacity of ≈372 mAh g⁻¹) anode, which dominates the battery market, is almost reaching its theoretical energy density and fails to meet the requirements (>350 Wh kg⁻¹) of current long-range electric vehicles.^[5] Therefore, there is an

urgent need to exploit “beyond LIBs” that can meet this demand.^[6–10] For the anode side, the lightweight (0.534 g cm⁻³), low electrochemical redox potential (−3.04 V vs standard hydrogen electrode), and high theoretical capacity (3860 mAh g⁻¹) of lithium make it an attractive candidate for the anode as an alternative to graphite.^[1,3,11–15] For the cathode side, in addition to exploring materials with a high capacity such as sulfur or oxygen, which bring additional problems caused by new materials, increasing the cut-off voltage is the most effective way to boost the energy density.^[3,4,6] Therefore, lithium metal batteries (LMBs) coupled with a high-voltage cathode are highly expected to be the next-generation battery systems.

However, the development of electrolytes has always lagged far behind electrodes and enormous attention is expected

to the development of electrolytes compatible with both the cathodes and anodes. Various electrolyte recipes have demonstrated great performance and among them, carbonate-based and ether-based electrolytes are the most used electrolytes. Despite that much higher Coulombic efficiency could be realized in ether-based electrolytes due to the formation of an elastic interface that helps withstand large volume changes of lithium during cycling,^[16] the cut-off voltages of the full cells are usually no more than 4.6 V even in high concentration electrolytes (HCEs) and localized high concentration electrolytes (LHCEs) because of the limited intrinsic electrochemical window of ethers, hindering their use in high-voltage battery systems.^[6,17–22] Moreover, the flash points of ethers are relatively low and gas generation occurs in ether-based electrolytes at a high voltage of ≈4.6 V even in a LHCE,^[23,24] making it unsuitable for very high voltage operation. Therefore, carbonate electrolytes with good oxidative stability and high flash points that have long been used in commercial LIBs are the most cost-effective and suitable to be adopted in high-voltage LMBs.^[25] However, conventional ethylene carbonate (EC)-based electrolytes are not stable against the lithium metal anode, forming a low-quality interface on it that leads to the uncontrolled growth of lithium, which aggravates the consumption of the electrolyte and eventually leads to battery failure.^[6,7,16] These EC-based electrolytes also undergo a series of side reactions with Ni-rich cathodes, including nucleophilic and dehydrogenation reactions, and ring-opening.^[4,6] The decomposition of lithium hexafluorophosphate (LiPF₆), the mainstream salt, is another critical issue of carbonate electrolytes because it

Z. Piao, R. Gao, Y. Liu, G. Zhou, H.-M. Cheng

Tsinghua-Berkeley Shenzhen Institute & Tsinghua Shenzhen International Graduate School

Tsinghua University

Shenzhen 518055, P. R. China

E-mail: cheng@imr.ac.cn

H.-M. Cheng

Faculty of Materials Science and Engineering/Institute of Technology for Carbon Neutrality

Shenzhen Institute of Advanced Technology

Chinese Academy of Sciences

Shenzhen 518055, P. R. China

The ORCID identification number(s) for the author(s) of this article can be found under <https://doi.org/10.1002/adma.202206009>.

DOI: 10.1002/adma.202206009

triggers parasitic side reactions that are more vigorous at high temperatures.^[26–28] In addition, the strong interaction between lithium ions (Li^+) and EC increases the de-solvation energy barrier, which is unfavorable for low-temperature applications.^[29] All these problems require a total rethink about the use of carbonate electrolytes for LMBs.

Fortunately, a large number of studies have contributed to developing high-performance carbonate electrolytes for LMBs, and the research indicates trends and principles that may be useful. However, there are only a few comprehensive reviews of carbonate electrolytes for LMBs, and they are mainly focused on the formation of a stable electrolyte/electrode interface rather than on the critical role of the Li^+ solvation structure in improving battery performance.^[7,30,31] We must emphasize that, on the one hand, it is essential to understand the relationship between the solvation structure and interface formation because the former has a significant impact on the latter; while on the other hand, lithium ions also undergo a series of processes during cycling including migration in the bulk elec-

trolyte, de-solvation at the interface, and encountering side reactions, all of which also highly rely on the solvation structure of Li^+ and are responsible for the battery performance (Figure 1).^[32] Also, when widening the operating temperature range of the batteries, the solvation structures have a more significant effect on the overall performance of the electrolyte. For example, LiPF_6 decomposition becomes more vigorous with increasing temperature while Li^+ migration and de-solvation become more sluggish at low temperatures,^[14,26,33,34] all of which are highly related to the solvation structure of Li^+ (Figure 1). Therefore, a systematic understanding of the solvation structure and its regulation strategies in LMBs can not only provide a timely overview of the latest developments in research but also provide guidance for rationally designing an electrolyte with outstanding performance in all respects.

In this review, we systematically summarize strategies for regulating the Li^+ solvation structure to boost the performance of carbonate electrolytes for LMBs. We first clarify key aspects of carbonate electrolytes including the properties of the components,

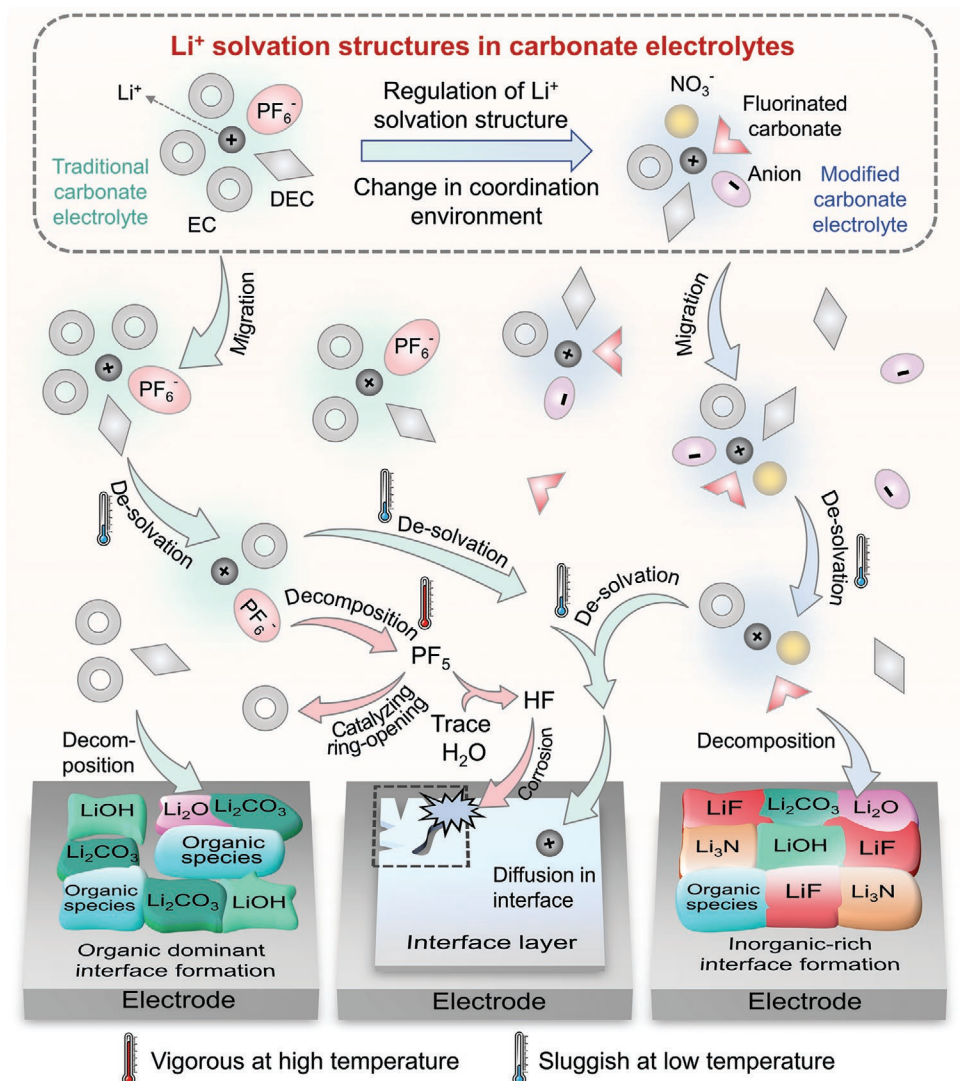


Figure 1. Schematic of Li^+ solvation structures and their behavior and reactions in a bulk electrolyte and at the interface.

the formation of Li^+ solvation structures, and critical Li^+ behavior in the electrolyte. We then consider the effects of four types of carbonate electrolytes with optimized solvation structures on Li^+ behavior and battery performance. We conclude with a summary of the current status of advanced carbonate electrolytes for LMBs and insight into future research regarding Li^+ solvation structures. The review provides guidelines for a better understanding of the science behind Li^+ solvation structures and Li^+ behavior to rationally design high-performance carbonate electrolytes for LMBs.

2. Key Aspects of Carbonate Electrolytes

To better understand and design a high-performance carbonate electrolyte, several key factors must be carefully considered. First are the physical properties, which highly determine the limitations of their use, including operating temperature and voltages, and also affect the solvation structure of Li^+ which further influences Li^+ behavior in the electrolytes. The Li^+ solvation structure of carbonate electrolytes and the factors that determine it are introduced for a better understanding of the resultant solvation structure. At the end of this section, several critical Li^+ behavior and their relationship with the solvation structure in carbonate electrolytes are illustrated.

2.1. Physical Properties of the Components in Carbonate Electrolytes

A general understanding of the properties of carbonate electrolytes can be obtained by comparing them with ether electrolytes which have also attracted great interest from academia and industry. First, the phase transition and flash points of carbonates are higher than those of ethers, indicating the low flammability of carbonate electrolytes.^[23] Second, they have superior oxidative stability against a high-voltage cathode as a result of the low highest occupied molecular orbital (HOMO) energy levels of carbonates (Table 1).^[35–41] However, their lowest unoccupied molecular orbital (LUMO) energy levels are also low (Table 1),^[40,41] resulting in their poor stability toward lithium metal anodes, which was a great challenge for their use in LMBs. In addition, carbonate electrolytes with low

donor numbers (DNs) have an inferior solubility for lithium salts, which explains why lithium nitrate (LiNO_3) is a common additive to ether electrolytes but has limited use in carbonate electrolytes.^[42–44]

As the overall properties of the electrolytes largely depend on the properties of their single components, including solvents and salts, these will be considered in detail next.

According to their configuration, carbonates typically fall into two categories, cyclic and linear (Figure 2a). Cyclic carbonates (including EC and propylene carbonate [PC]) have large dielectric constants and occupy the inner layer of the solvation structure in the electrolyte (Figure 2b).^[41,45] A high dielectric constant also increases the dipole–dipole force between molecules, resulting in an increase in the phase transition point and viscosity of the electrolyte.^[23] Linear carbonates (including dimethyl carbonate [DMC], diethyl carbonate [DEC], and ethyl methyl carbonate [EMC]) with relatively small dielectric constants are less dominant in the Li^+ solvation structure. Due to the weaker dipole–dipole force, their phase transition point and viscosity are lower than those of cyclic carbonates. One should note that the viscosity of the electrolyte increases drastically at low temperatures and affects the de-solvation process of Li^+ , which is the rate-determining step of the charge transfer of the electrolyte at low temperature.^[32,46] Thus, linear carbonates are more conducive for low-temperatures because their low melting point and low viscosity ensure the electrolyte remains liquid phase with good charge transfer kinetics at low temperatures. Conversely, cyclic carbonates are better for high-temperature applications because of their high flash and phase transition points. As verified experimentally, by using EC and PC as the main solvents in the electrolyte, the battery can work stably at a high temperature of 80 °C, far exceeding the operating temperatures of conventional electrolytes.^[47]

As fluorination becomes an emerging strategy to improve the properties of molecules as electrolyte components, more and more fluorinated carbonates have joined the family of carbonates, including the EC-based fluorinated derivative, fluoroethylene carbonate (FEC), and the EMC-based fluorinated derivative methyl(2,2,2-trifluoroethyl)carbonate (FEMC) (Figure 2a).^[51–56] The incorporation of fluorine with a strong electronegativity lowers the HOMO and LUMO energy levels of the base solvents, resulting in easier reduction at the anode to form a lithium fluoride (LiF)-rich solid electrolyte interface

Table 1. Physical properties of representative carbonates and ethers.

Solvent	LUMO [eV]	HOMO [eV]	Melting point, T_m [°C]	Boiling point, T_b [°C]	Flash point, T_f [°C]	Dielectric constant, ϵ
EC (ethylene carbonate)	1.089	-7.924	36.4	248	160	89.78
PC (propylene carbonate)	1.112	-7.870	-48.8	242	132	64.9
DMC (dimethyl carbonate)	1.189	-7.718	4.6	91	0.76	3.11
DEC (diethyl carbonate)	1.254	-7.633	-74.3	126	31	2.81
EMC (ethyl methyl carbonate)	1.222	-7.675	-53	110	23	2.96
FEC (fluoro-ethylene carbonate)	0.696	-8.315	20	210	102	78.4
DME (1,2-dimethoxy ethane)	2.532	-6.695	-58	82.5	0	5.5
DOL (1,3-dioxolane)	3.049	-6.639	-97.2	75.6	1	6.74
TEGDME (tetraethylene glycol dimethyl ether)	2.186	-6.613	-45	216	106	7.9

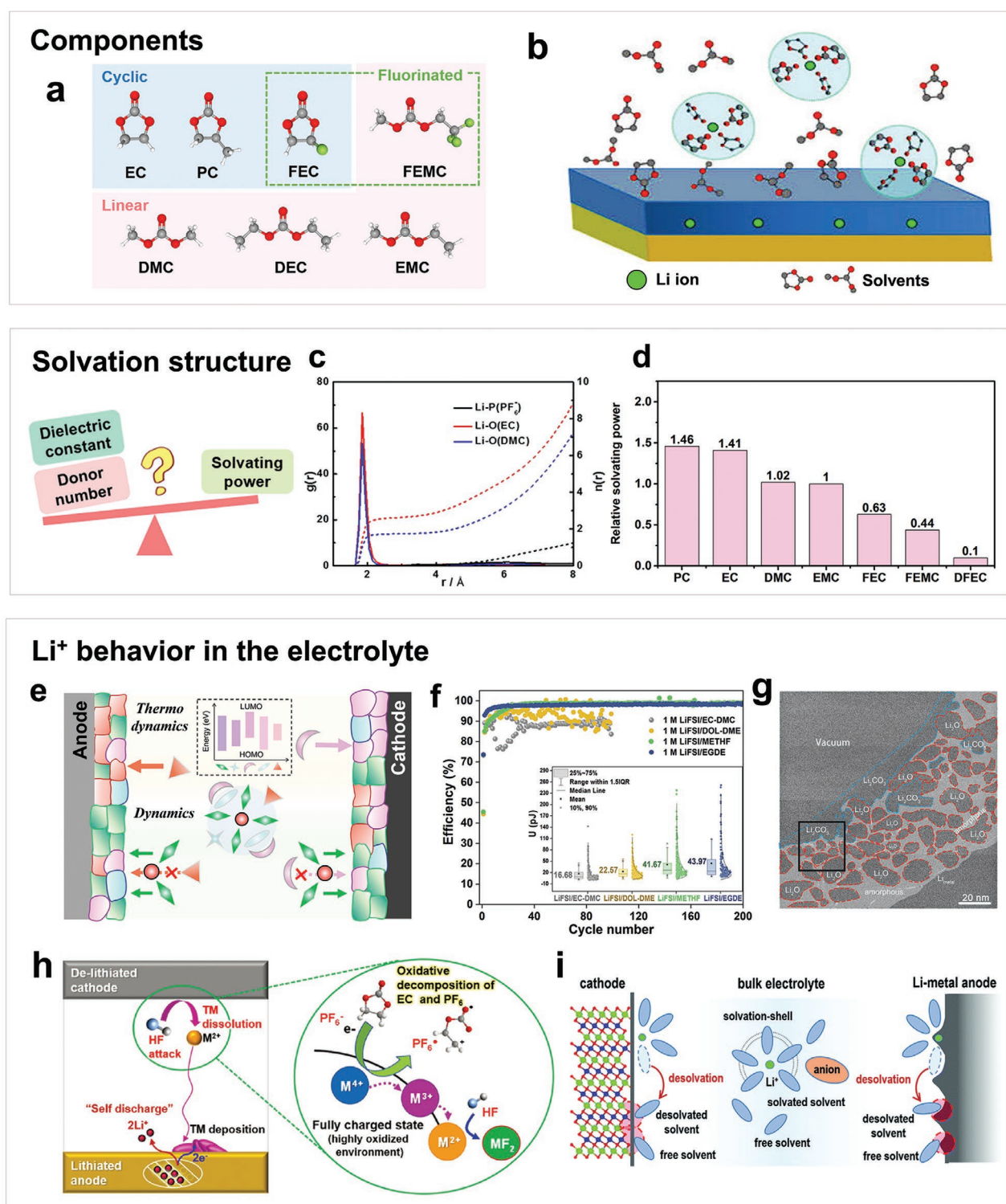


Figure 2. Key aspects of carbonate electrolytes. a) Chemical structure of representative carbonate solvents. b) Schematic of the solvation structure of Li^+ in a carbonate electrolyte. Reproduced with permission.^[45] Copyright 2012, Springer Nature. c) Calculated radial distribution functions ($g(r)$, solid lines) and coordination numbers ($n(r)$), dash lines for an EC-based electrolyte (1 M LiPF_6 in EC/DMC [1:1 v/v]). Reproduced with permission.^[48] Copyright 2021, American Chemical Society. d) Solvating power series of common carbonate solvents. e) Schematic of interface formation determined by thermodynamic and dynamic features. f) Comparison of the cyclic performance of Li metal anodes in carbonate and ether electrolytes. The inset shows the maximum elastic deformation energy (U) of SEIs formed in electrolytes. Reproduced with permission.^[46] Copyright 2021, Elsevier. g) Cryogenic transmission electron microscopy images and schematic of the SEI structure in an EC-based electrolyte (1 M LiPF_6 in EC/DEC [1:1 v/v]). Reproduced with permission.^[49] Copyright 2021, Wiley-VCH. h) HF-triggered failure mechanisms. Reproduced with permission.^[26] Copyright 2018, Wiley-VCH. i) Schematic of the de-solvation process at interfaces on both electrodes. Reproduced with permission.^[50] Copyright 2020, Royal Society of Chemistry.

(SEI) and improved stability against the high-voltage cathode, which effectively retards the consumption of electrolyte and extend the lifespan of batteries.^[55] In addition, fluorinated components facilitate the de-solvation of Li⁺ at both electrodes due to their weakened interaction with Li⁺.^[53]

Except for solvents, salts are also crucial components of the electrolyte. LiPF₆ is the mainstream lithium salt in dilute carbonate electrolytes with overall acceptable properties in terms of electrochemical stability, solubility, ionic conductivity, etc.^[57] However, serious LiPF₆ decomposition occurs in LiPF₆-containing electrolytes, especially at high temperatures.^[58] Blending LiPF₆ with thermally stable lithium salts such as lithium difluoro(oxalate)borate (LiDFOB) and lithium bis(oxalato)borate improves the high-temperature stability of the electrolyte.^[47] However, their low solubility has hindered their use as the main salts of carbonate electrolytes and LiDFOB is more used as an additive.^[34,59–61] Lithium bis(trifluoromethanesulfonyl)imide (LiTFSI) and lithium bis(fluorosulfonyl)imide (LiFSI) are alternative Li salts in carbonate electrolytes, but they corrode the current collector of the cathode aluminum (Al) at high voltages, restricting their use in dilute carbonate electrolytes.^[62] Fortunately, it is avoided in HCEs and LHCEs without free solvents dissolving Al³⁺,^[63] thus along with the desirable solubility and film-forming capability of LiTFSI and LiFSI, they have been extensively investigated in HCEs and LHCEs.^[64,65] Whereas, LiPF₆ does not have this problem even in dilute electrolytes since it forms a stable inert layer on the surface of the Al current collector and thus suppresses the corrosion of Al at high voltages.^[66,67]

To summarize, different components in carbonate electrolytes have distinctive properties and no single component can meet all the requirements of different scenarios. Therefore, a rational screening and blending of the components to obtain a new solvation structure is essential to take advantage of the different components to achieve a balanced electrolyte.^[64,68]

2.2. Formation of Li⁺ Solvation Structure in Carbonate Electrolytes

In non-aqueous carbonate electrolytes, there is a strong interaction between Li⁺ and carbonate solvents, forming a Li⁺ solvation structure. A recent comprehensive review by Cheng et al. highlighted the critical role of the solvation structure in electrolytes for LIBs.^[69] Some aspects of this are applicable to LMBs that the solvation structure not only contributes to the formation of the interface, but also affects ionic conductivity, Li⁺ transference number (t_+), liquid temperature range, de-solvation process, etc.^[69–71] It is therefore very important to understand the solvation structure of Li⁺ in the electrolyte. Fortunately, a basic understanding of the solvation structure of electrolytes has been provided by theoretical calculations and characterization methods.^[72]

The solvation structure is derived from the competitive coordination of solvents and anions with Li⁺ and is determined by many factors. The polarity of the components is one of the factors that affect their coordination with Li⁺.^[73] In conventional carbonate electrolytes, the salt anions are less prone to be solvated by Li⁺ due to the strong dipole–ion interaction between

Li⁺ and the solvent. As mentioned above, cyclic carbonates with a large dielectric constant extensively coordinate with Li⁺ to dominate the inner layer of the solvation structure, whereas linear carbonates with a small dielectric constant are usually repelled to the outer layer of the solvation structure (Figure 2c). The DN value is also considered to be a factor determining the solvation structure of Li⁺. For example, nitrate ions (NO₃[−]) have a high DN and thus normally occupy the inner layer of the solvation structure of Li⁺.^[74,75] However, Su et al. argued that none of these two parameters can accurately determine the solvation structure of Li⁺, because both haven't taken into account the steric hindrance and chelate effects. They proposed a new descriptor to more precisely determine the interaction of the target molecule with Li⁺ (Figure 2d). According to the results, the interaction of molecules with Li⁺ becomes weaker after fluorination, which is consistent with the general perception.^[53] Such a decrease in the interaction between solvent and Li⁺ leads to more anions participating in the inner layer of the solvation structure.^[70] In addition to the nature of the individual components, the concentration of the electrolyte also has a large effect on the solvation structure of Li⁺. As the concentration increases, anions with increasing proportions in the electrolyte are forced to enter the inner solvation structure of Li⁺, forming a solvation structure dominated by anions.

Although we have a general understanding of the Li⁺ solvation structure and the factors that influence it, there are no effective tools to observe the changes in the solvation structure in the bulk and interface during cycling, and currently there is no powerful way of helping us accurately predict the solvation structure, and this requires more research.

2.3. Li⁺ Behaviors in Carbonate Electrolytes

Li⁺ undergoes a series of processes in the electrolyte. After being solvated, the solvation structure of Li⁺ migrates under the electric field, and de-solvates when reaching the interfaces between the electrodes and the electrolyte, followed by forming interface layers from the decomposition of components and Li⁺ diffuses through them before reaching the electrodes. In addition to interfaces, some specific components in the solvation structure decompose in the bulk electrolyte as well. All above Li⁺ behaviors are highly determined by solvation structure, among which forming a stable interface has attracted the most research interest.

The formation of the interface is mainly determined by two factors: thermodynamically, components with lower LUMO and higher HOMO energy levels are more likely to decompose at the electrodes to form interface layers; dynamically, the components that are more prone to contact the electrodes may preferentially decompose at the electrodes, and this is highly related to the solvation structure (Figure 2e).^[76] Because the complexation with electron-withdrawing Li⁺ reduces the LUMO energy levels of the components, those dominating the inner layer of the solvation structure are more likely to be reduced on the anode to form interfaces. For the cathode side, while an electrolyte with a low HOMO is generally considered to be oxidatively stable, Zou et al. proposed a new interfacial model where the decomposition of components is highly determined by their

distance from the cathode.^[77] It is therefore necessary to carefully consider both thermodynamic and dynamic factors to construct favorable interfaces.

In conventional carbonate electrolytes, EC dominates the inner layer of the Li⁺ solvation structure while PF₆⁻ is repelled away from Li⁺, which makes EC preferentially contact the anode to decompose, forming a weak SEI rich in lithium carbonate (Li₂CO₃), lithium ethylene dicarbonate, and lithium ethylene mono-carbonate.^[7,30,78,79] It is found that the mechanical properties of the SEI formed in carbonate electrolytes are far worse than those formed in ether electrolytes, resulting in lower Coulombic efficiency of the cells (Figure 2f).^[16] Han et al. examined the SEI formed in the conventional EC/DEC electrolyte using cryo-electron microscopy and found that the Li₂CO₃ in the SEI continues to react with the electrolyte, leading to poor stability of the interface layer (Figure 2g).^[49] It is therefore necessary to change the Li⁺ solvation structure to improve the SEI in carbonate electrolytes.

Compared to interfaces rich in organics, the formation of inorganic-rich interfaces is preferable for developing high-performance LMBs. Among these, a lithium nitride (Li₃N)-rich interface is one of the most powerful inorganic SEI components that can effectively regulate the morphology of the lithium deposit thanks to its superior ionic conductivity.^[80] LiF is another desirable SEI component because of the following: 1) the large interfacial energy of LiF with lithium metal is conducive to the lateral movement of Li⁺ on the interface, which inhibits the perpendicular growth of lithium dendrites;^[81] 2) its poor electrical conductivity prevents electronic tunneling which inhibits continuous electrolyte consumption.^[64,82-86] Moreover, an in situ LiF interface is believed to better protect the electrode compared with the ex situ LiF interface since in situ LiF is capable of maintaining a more uniform interface during cycling.^[87] Nonetheless, the state and the role of LiF in the interface layers are controversial because Huang et al. argue that LiF does not enter the interface layer, but segregates to form nanoparticles on the electrode.^[88]

In addition to the formation of stable interfaces, with the extension of the operating temperature, the impact of Li⁺ behavior and reactions in the electrolytes on the battery performance becomes more significant. For example, at high temperatures, the LiPF₆ in the electrolyte suffers serious decomposition. Since Li⁺ with a large charge-to-radius ratio can easily separate fluorine from PF₆⁻, ion-paired LiPF₆ without complete dissociation can be easily decomposed into phosphorus pentafluoride (PF₅) and LiF.^[26] The generated PF₅ not only catalyzes the ring-opening reaction of cyclic carbonates to form carbonate polymers at the interface,^[26,33] but also reacts with trace water to generate aggressive hydrogen fluoride (HF) which destroys the integrity of the interface and triggering various parasitic side reactions (Figure 2h).^[58] Fortunately, the decomposition can be suppressed by regulating the solvation structure of Li⁺. Kawamura et al. explored the relationship between the LiPF₆ decomposition and the surrounding of Li⁺ in the electrolyte. They found that the decomposition reaction rate decreases with the increasing dielectric constant of the solvent due to the enhanced dissociation of LiPF₆, which is undesirable for LiPF₆ decomposition.^[89] Nevertheless, the suppression of LiPF₆ decomposition has not received as much attention in LMBs as that in LIBs.^[28,89,90] When reaching the

low-temperature regime, with the dramatic increase of the viscosity of the electrolyte, the ionic conductivity and de-solvation kinetics which are highly determined by the Li⁺ solvation structure become dominant factors affecting the kinetics of the battery.^[14,34] If free solvents remaining near the interface after de-solvation are electrochemically unstable, they can be decomposed and decrease the battery performance (Figure 2i).^[50] Therefore, it is important to develop a solvation structure that is not only able to induce the formation of inorganic-rich stable interfaces but also stable and kinetically favorable in the bulk electrolyte and against both electrodes.

3. Design of High-Performance Carbonate Electrolytes

After understanding the above key aspects, a better carbonate electrolyte can be produced. Because the Li⁺ solvation structure is a result of the competitive coordination of different solvents and anions with Li⁺, it can be reshaped by modifying the coordination configuration of Li⁺. In this section, strategies involving the manipulation of the solvation structure are summarized and divided into four main categories: advanced carbonate electrolytes with special additives, a high DN anion dominant structure, a salt anion dominant solvation structure, and a fluorinated carbonate dominant solvation structure. A combined effect brought by “cocktail strategy” is also discussed at the end of this section.

3.1. Modified Carbonate Electrolytes with Special Additives

Developing advanced carbonate electrolytes by adding special chemicals is the most economical strategy to improve the performance of LMBs. For LMBs, considering the low Coulombic efficiency of the Li||Cu cells with conventional baseline electrolytes,^[52,74,75,48,91,92] most reports on additives have contributed to increasing the Coulombic efficiency by constructing stable interface layers on the anode. Most of these have low LUMO values and thus undergo preferential decomposition to form a high-quality interface on the lithium metal anode, such as LiNO₃ which will be discussed specifically in Section 3.2. Currently, except for LiNO₃, more and more research is being devoted to developing multi-functional additives with novel functions, not limited to optimizing the interface at the anode.^[93]

An extensive number of studies have reported additives that optimize the interfaces at both electrodes. As mentioned before, an agent with a low LUMO and high HOMO energy level will decompose at both electrodes to form interface layers. LiDFOB is a typical additive with this feature and its electrochemical window is within the range of that of most solvents and salts, so it is considered a promising additive for high-voltage LMBs. When a little amount of LiDFOB is introduced to the electrolyte, it forms interfaces rich in LiF and B-containing oligomers at both electrodes and it is proved to be an effective strategy to improve the high-voltage performance of the batteries.^[27,94-97] It is also reported that LiDFOB helps form a uniform film composed of evenly distributed nanostructured LiF particles due to the capping ability of its oxalate moiety, and this results in uniform diffusion field gradients on the electrode

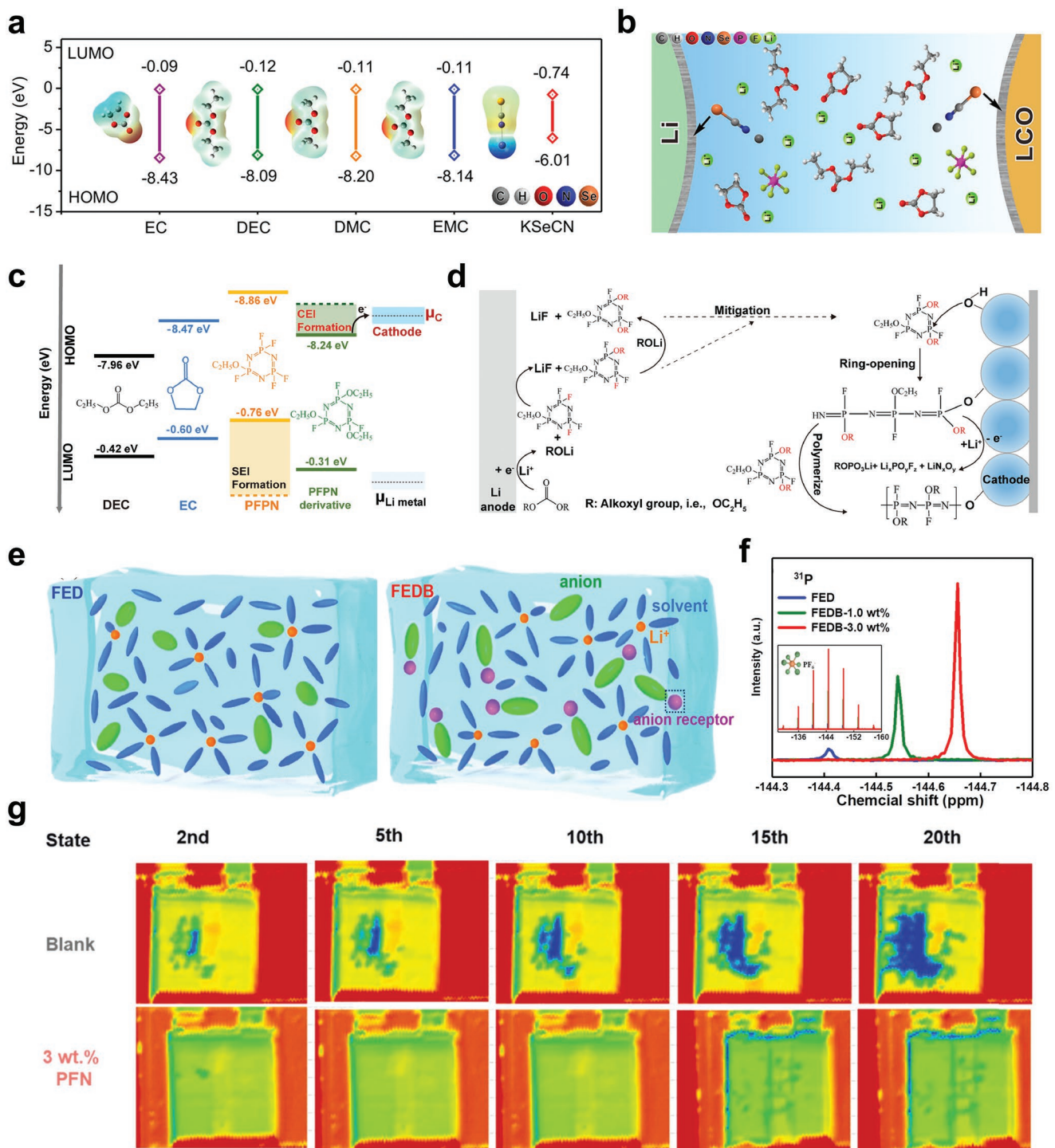


Figure 3. Characteristics and performance of carbonate electrolytes modified with special additives. a) Calculated LUMO and HOMO values of conventional carbonate solvents and KSeCN. b) Schematic of how KSeCN behaves to stabilize the interface of a Li metal anode and LCO cathode. a,b) Reproduced with permission.^[99] Copyright 2022, American Chemical Society. c) Frontier molecular orbital levels of carbonate solvents (EC and DEC), PFPN, and a PFPN derivative. d) Possible decomposition reactions of PFPN occurring on the Li anode and the high-voltage cathode. c,d) Reproduced with permission.^[102] Copyright 2021, Elsevier. e) Schematics of the electrolyte solvation structures and f) ³¹P NMR spectra of the electrolytes before and after the addition of an anion receptor. Reproduced with permission.^[103] Copyright 2021, Wiley-VCH. g) Ultrasonic images of NCM811||Li cells during cycling in blank and PFN-containing electrolytes. Reproduced with permission.^[27] Copyright 2022, Elsevier.

to improve cycling performance.^[98] There are many other additives possessing similar features. Fu et al. used potassium selenocyanate (KSeCN) as a multi-functional additive for LiCoO₂

(LCO)||Li batteries. Because of its low LUMO and high HOMO values, KSeCN preferentially decomposes at both electrodes to form protective layers (Figure 3a,b), enabling a LCO||Li cell to

maintain a high capacity of 129 mAh g⁻¹ after 940 cycles at a cut-off voltage of 4.6 V.^[99] Similarly, hexafluoroisopropyl trifluoromethanesulfonate with low LUMO and high HOMO values induces the formation of stable interfaces at both electrodes.^[100] In addition, Zhou et al. modulated both interfaces by using *N,N*-diethyl-2,3,3,3,-tetrafluoropropionamide (DETPF) with low LUMO and high HOMO values as an additive. The LiFePO₄||Li cell with DETPF exhibited extraordinary capacity retention of 92.7% after 800 cycles even at a high rate of 5 C.^[101]

One should note that a high HOMO value is not necessary for the additives to form a stable interface at the cathode. For example, Liu et al. used fluorinated cyclophosphazene (PFPN) as an additive to optimize the interfaces at both electrodes. Although this additive itself does not have a high HOMO value, the PFPN derivatives in situ generated during cycling have high HOMO values and so can be oxidized at the cathode to produce a robust P, N-rich cathode electrolyte interface (CEI) (Figure 3c,d). As a result, the capacity retention of a LiNi_{0.5}Mn_{1.5}O₄||Li battery was 90.7% after 100 cycles at an extremely high cut-off voltage of 4.9 V.^[102] Due to the dynamic feature of interface layers in composition and structure during cycling, even if the Coulombic efficiency rises to a high level in the first few cycles with the formation of stable interface layers, those sacrificial additives continue to play a role in maintaining the integrity and stability of the interface layers on both electrodes until being consumed completely so that the Coulombic efficiency could remain to be high for long life.

Some additives can also produce high-quality interfaces without being decomposed. Huang et al. introduced the anion receptor tris(trimethylsilyl) borate (TMSB) to carbonate electrolytes, where its electron-deficient center borate has a strong interaction with anions (Figure 3e). The molecular dynamics (MD) simulation results show that TMSB tends to adsorb on the surface of lithium metal and accumulate in the electric double layer region, attracting anions close to the lithium anode, which in turn induces the decomposition of anions to form an inorganic-rich SEI. As the attracted anions get close to the anode, they attract Li⁺ by electrostatic forces to form an anion dominant Li⁺ solvation structure at the interface (which will be discussed in Section 3.3 in detail), and this phenomenon indicates that the solvation structures at the interface and in the bulk may be different.^[103]

In addition to optimizing the interfaces, some additives can also improve Li⁺ migration and de-solvation processes. Wu et al. found that a tris(4-fluorophenyl)phosphine (TFPP) additive decreases the coordination number of EC in the Li⁺ first solvation shell because negatively charged F in TFPP strongly interacts with Li⁺ to replace the EC.^[104] It has been reported that the introduction of specific anions like Br⁻ also reduces the amount of solvent in the solvation structure, thereby reducing the de-solvation energy barrier.^[105] What's more, anion receptor additives can significantly increase t₊ since they attract anions and weaken the interaction between the anions and Li⁺ (Figure 3f).^[103]

There are also additives with novel functions including scavenging HF formed by LiPF₆ decomposition. Zhang et al. compared ultrasonic images of a LiNi_{0.8}Co_{0.1}Mn_{0.1}O₂ (NCM811) ||Li battery during cycling before and after adding an ethoxy(pentafluoro)cyclotriphosphazene (PFN) additive, and

found that after introducing the additive, the pouch cell had less gas accumulation (Figure 3g), which greatly improved its thermal stability.^[27]

In brief, additive regulations are the most cost-effective way to improve the Li⁺ behavior in carbonate electrolytes from many aspects and these are not limited to forming stable interfaces. Additives with low LUMO and high HOMO values are thermodynamically driven to decompose to form interfaces at both electrodes to prevent the further decomposition of electrolytes. There are also processes that are dynamically driven. For example, anion receptors can attract anions to contact the interface to form an anion-induced interface. In addition to constructing stable interface layers, some multi-functional additives improve the battery performance from many different aspects including increasing t₊, lowering the de-solvation energy barrier, and alleviating side reactions. Although there are many kinds of additives with novel functions, it is necessary to combine them with other strategies to improve the overall performance considering the limited amount of additives in the electrolyte.

3.2. Modified Carbonate Electrolytes with a Solvation Structure Dominated by High DN Anions

In recent years, LiNO₃ has received extensive attention as an additive so we shall consider it separately to discuss the critical role of NO₃⁻ in carbonate electrolytes. The high DN (22) and dielectric constant cause NO₃⁻ to occupy the inner layer of the Li⁺ solvation structure; at the same time, it has a low LUMO energy level, so that NO₃⁻ is prone to be reduced at the anode to form an anion-induced highly conductive Li₃N-rich interface.^[42,106] Compared with the interface formed by the decomposition of solvents in conventional carbonate electrolytes, an anion-induced inorganic-rich interface has a wider band gap, higher ionic conductivity, and better mechanical properties, which makes it effective at inhibiting electron tunneling, homogenizing Li⁺ flux, and adapting to the volume change of electrodes. However, the high DN value of anions also brings challenges. Due to its strong interaction with the Lewis acid Li⁺, it is difficult for LiNO₃ to be dissociated in the electrolyte, resulting in low solubility in carbonate electrolytes.

A lot of recent research has been devoted to improving the solubility of NO₃⁻ in carbonate electrolytes. The most commonly used strategy is to introduce co-solvents to compete with NO₃⁻ for coordination with Li⁺. Most reported co-solvents have high DNs including ethers like tetraethylene glycol dimethyl ether (DN = 17),^[107] dimethyl ether (DN = 20),^[108,109] crown ether,^[110] diglyme (DN = 19.5),^[111] and other co-solvents like dimethyl sulfoxide (DN = 29.8),^[42] tris(pyrrrolidinophosphine) oxide (TPPO, DN = 47.2),^[75] and tetramethylurea (TMU, DN = 31),^[74] which can competitively coordinate with Li⁺ thereby separating Li⁺ and NO₃⁻. A high DN value is, however, not necessary for solvents to dissolve LiNO₃. Piao et al. used sulfolane with a low DN value but high polarity as a co-solvent to dissolve LiNO₃,^[48] and Zhao et al. successfully dissolved 0.7 M LiNO₃ in EC as the solvent, which also has a high polarity but low DN value (Figure 4a).^[112] Yang et al. demonstrated that low-polarity ethylene glycol diacetate (EGD, ϵ = 7.7) is also capable of dissolving LiNO₃. In this

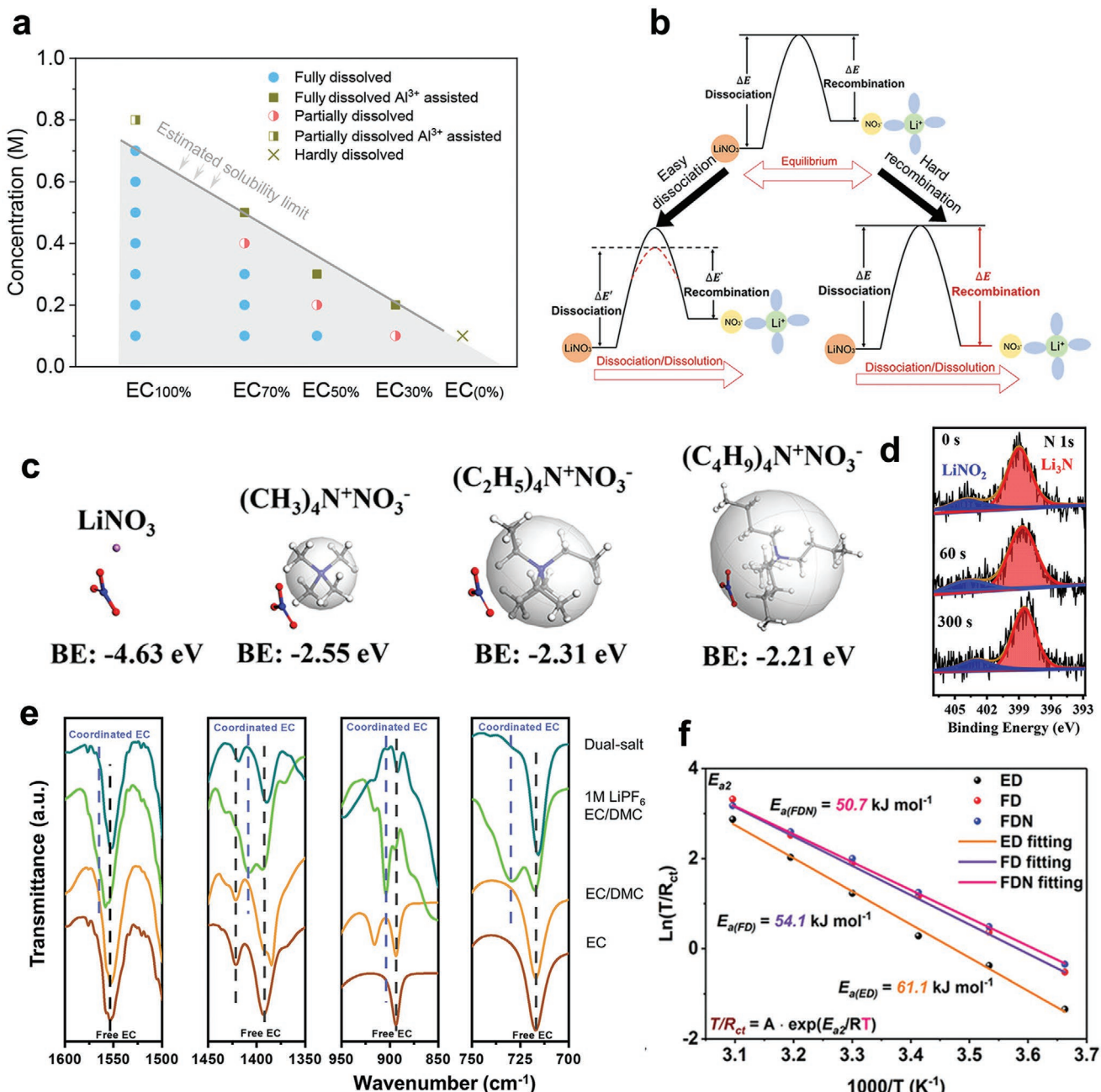


Figure 4. Strategies of introducing NO_3^- in carbonate electrolytes and the characteristics of carbonate electrolytes with a NO_3^- dominant solvation structure. a) Solubility map for LiNO_3 in carbonate electrolytes. Reproduced with permission.^[112] Copyright 2022, Wiley-VCH. b) Schematic of the equilibrium between dissociation and recombination. The equilibrium state between dissociation and recombination and increasing the solubility of LiNO_3 produced by preventing the recombination of Li^+ and NO_3^- . Reproduced with permission.^[113] Copyright 2021, American Chemical Society. c) Molecular formulas and binding energies of LiNO_3 and tetramethylammonium nitrate with different sizes of cations. d) N 1s spectra of the surface of the Li metal anode in $\text{Li}||\text{Li}$ cells after ten cycles with an electrolyte containing $\text{R}_4\text{N}^+\text{NO}_3^-$. c,d) Reproduced with permission.^[106] Copyright 2022, American Chemical Society. e) FTIR spectra of some selected characteristic peaks. Reproduced with permission.^[107] Copyright 2021, American Chemical Society. f) Nyquist plots and activation energies of Li^+ de-solvation in $\text{Li}||\text{Li}$ cells after three cycles at different temperatures with different electrolytes. Reproduced with permission.^[108] Copyright 2021, Wiley-VCH.

case, the uncoordinated carbonyl groups of EGD repel NO_3^- by electrostatic forces, thus inhibiting the recombination of Li^+ and NO_3^- (Figure 4b), so that 0.3 M LiNO_3 was successfully dissolved with the addition of EGD.^[113] The introduction of Lewis acid anions is another strategy to dissolve LiNO_3 in carbonate

electrolytes without any co-solvent. Density functional theory (DFT) indicates that the electron-deficient B center in BF_4^- tends to interact with the electron-rich N in NO_3^- , which helps dissociate Li^+ and NO_3^- . With the addition of BF_4^- , in addition to forming a Li_3N -rich SEI, an F, B-rich CEI is formed on the

cathode. As a result, NCM811||Li cell with a high loading using the electrolyte containing BF_4^- has a high capacity retention of 80.3% after cycling for 250 cycles.^[114] In addition to the above strategies, changing the cations of LiNO_3 has been shown to effectively dissolve NO_3^- in carbonate electrolytes. When the Li^+ is replaced by a large cation like quaternary ammonium (R_4N^+) with a delocalization state of positive charge, the binding force between the anion and the cation is weakened, which is favorable for dissociating cations and NO_3^- in carbonate electrolytes, producing more of the NO_3^- -derived SEI (Figure 4c,d).^[106] In addition, some studies dissolve LiNO_3 by introducing a covalent organic framework,^[115] metal organic framework,^[116] and other coatings.^[117] It has also been reported that LiNO_3 can be directly embedded on the lithium metal anode to form a salt-in-metal anode using a mechanical kneading approach.^[118]

In addition to stabilizing the interface, the introduction of NO_3^- also reduces the content of solvents in the inner layer of the solvation structure to promote the de-solvation of Li^+ . As shown in Figure 4e, the characteristic peaks of coordinated EC in Fourier transform infrared (FTIR) spectroscopy are weakened after the introduction of LiNO_3 , implying weakened

interaction between Li^+ and solvents.^[107] Wang et al. also found that the de-solvation energy barrier is significantly reduced after the addition of NO_3^- (Figure 4f).^[108] Liu et al. attributed the increase in exchange current during lithium deposition process to the improved Li^+ de-solvation process which stems from the replacement of solvents in the inner solvation structure by NO_3^- .^[117] These results consistently indicate that NO_3^- can change the interaction between solvents and Li^+ , thereby improving the de-solvation kinetics.

An additional merit of introducing NO_3^- to the solvation structure would be the improvement of the thermal stability of LiPF_6 -containing electrolytes. Because the anions are also repelled to the outer layer of the solvation structure by the incorporation of NO_3^- , LiPF_6 decomposition is inhibited due to the weakened interaction between Li^+ and PF_6^- , which contributes to an improvement of the high-temperature performance. Xiao et al. introduced LiNO_3 and TPPO co-solvents into a conventional carbonate electrolyte. Due to the strong Lewis basicity of NO_3^- and TPPO as well as the large molecular size of TPPO, PF_6^- ions are repelled in the solvation structure as proven by MD simulation results (Figure 5a,b), weakening the $\text{Li}^+-\text{PF}_6^-$

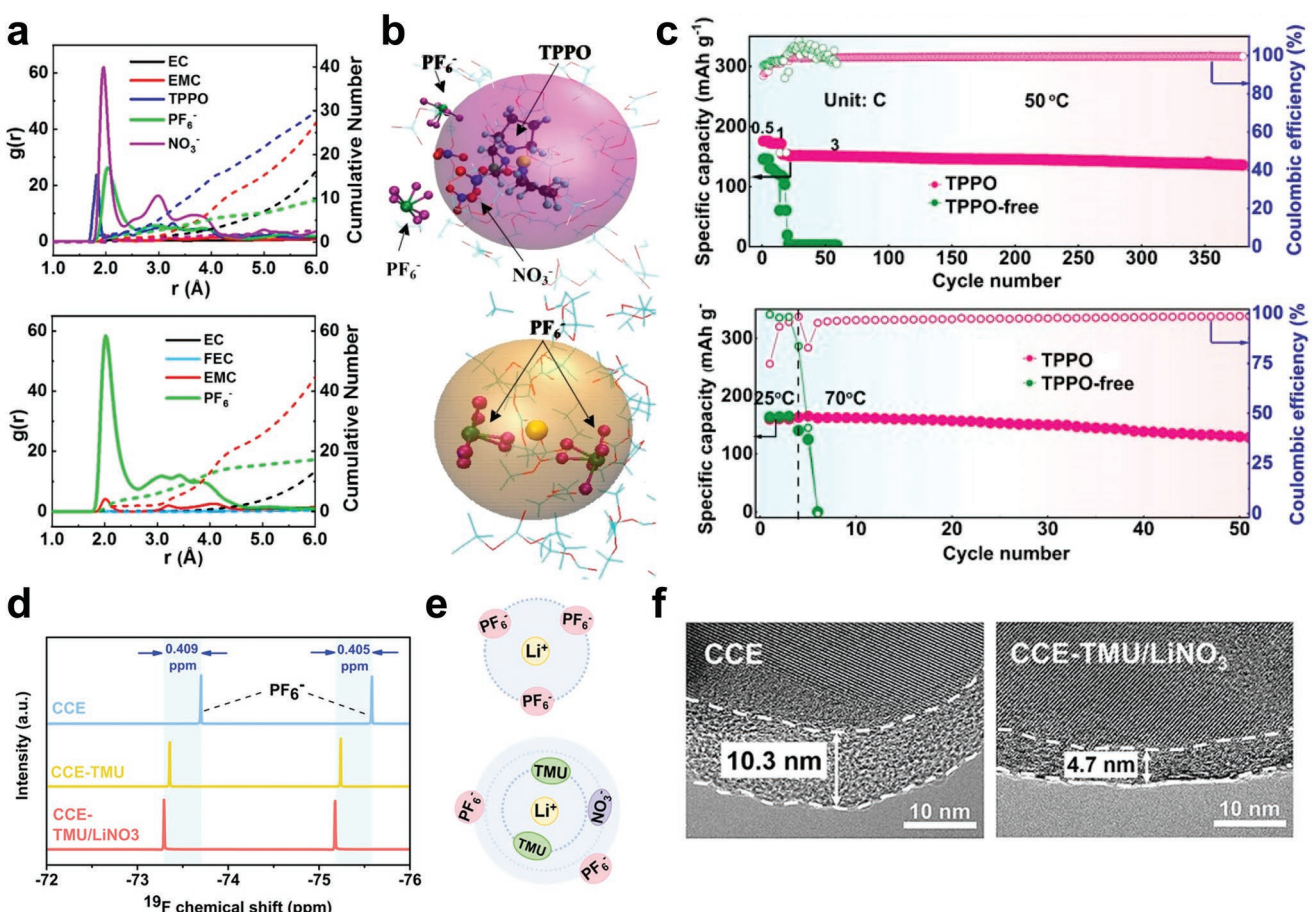


Figure 5. Suppression of LiPF_6 decomposition in carbonate electrolytes with a NO_3^- dominant solvation structure. a) Radial distribution function ($g(r)$, solid line) and cumulative number (dashed line) of Li^+ in electrolytes with and without LiNO_3 . b) Representative solvation shells of lithium ions in electrolytes with and without LiNO_3 . c) Rate and cycling performance $\text{LiFePO}_4||\text{Li}$ cells in different electrolytes at high temperatures of 50 and 70 °C, respectively. a–c) Reproduced with permission.^[75] Copyright 2021, American Chemical Society. d) ¹⁹F NMR spectra of different electrolytes. e) Representative configurations of the solvation structures of Li^+ in electrolytes before and after the addition of LiNO_3 . f) High-resolution transmission electron microscopy images of the CEIs formed in electrolytes before and after the addition of LiNO_3 . d–f) Reproduced with permission.^[74] Copyright 2022, Wiley-VCH.

interaction and thus inhibiting LiPF_6 decomposition. As a result, the $\text{LiFePO}_4\text{||Li}$ cells can stably cycle for 350 cycles at 3 C at 50 °C and 50 cycles at 0.3 C at a temperature of 70 °C which is high for such a battery, while the cells with the traditional carbonate electrolyte failed in few cycles (Figure 5c).^[75] Similar effects have been achieved by introducing a TMU co-solvent and LiNO_3 additives. Despite the small size of the TMU, the distance between Li^+ and PF_6^- is increased because of its strong Lewis basicity as shown by nuclear magnetic resonance (NMR) spectroscopy and MD simulation results (Figure 5d,e). Because of this, the generation of HF is suppressed, which alleviates the destruction of interfaces and electrolyte decomposition during cycling, indicated by a significant reduction of the thickness of the CEI after cycling (Figure 5f).^[74]

To summarize, NO_3^- as a representative of high DN anions in carbonate electrolytes, occupies the inner layer of the solvation structure and because of its low LUMO value it can be preferentially reduced to form a conductive Li_3N -rich interface at the anode, regulating Li^+ flux further inhibiting the growth of lithium dendrites. The introduction of NO_3^- can also weaken the interaction between Li^+ and solvent as well as with anions, thus promoting the de-solvation process and inhibiting the thermal decomposition of LiPF_6 . Though the strong interaction between Li^+ and NO_3^- restricts its solubility in carbonate electrolytes, many studies have been devoted to improving the solubility of NO_3^- thus producing a significant improvement of the battery performance. Future research should focus on improving the compatibility between the NO_3^- dominant solvation structure and the high voltage cathode to overcome the inherently inferior oxidation stability of NO_3^- .

3.3. Modified Carbonate Electrolytes with a Solvation Structure Dominated by Salt Anions

As discussed in Section 3.2, the introduction of functional anions to the solvation structure can induce the decomposition of anions to form an inorganic-dominated interface. An anion-dominant solvation structure can also be obtained by regulating the competitive coordination of solvents and salt anions without the addition of special anions. There are two ways to obtain a solvation structure dominated by salt anions: one is to force more salt anions to coordinate with Li^+ by increasing the concentration of the electrolyte, and the other is to decrease the coordination of solvents with Li^+ by weakening the interaction between them.

As concentration increases, the number of anions in the inner solvation structure also increases, leading to the HOMO and LUMO energy levels of the overall electrolyte decreasing to those of the salt. This promotes the prior decomposition of the salt anions at the anode instead of solvents, and the oxidation resistance of the electrolyte against the cathode is also increased. Fan et al. reported an HCE of 10 M LiFSI in EC/DMC and found that FSI^- is preferentially decomposed at the anode, forming a LiF-rich SEI. Also, as the content of the solvent decreases, FSI^- plays a dominant role in the formation of a fluorinated CEI on the Ni-rich cathode (Figure 6a). As a result, the capacity retention rate of a $\text{LiNi}_{0.6}\text{Co}_{0.2}\text{Mn}_{0.2}\text{O}_2$ (NCM622) || Li cell is as high as 86% after 100 cycles at a high

cut-off voltage of 4.6 V.^[119] Subsequent research by Liu et al. came to the same conclusion. They reported an HCE of 6.5 M LiFSI in EC/DMC and a decrease in the HOMO energy level of the HCE with increasing concentration was verified by DFT calculation results (Figure 6b). As a result, a NCM622 || Li cell with this HCE had a higher initial Coulombic efficiency than the baseline dilute electrolyte at a cut-off voltage of 4.6 V, implying less irreversible decomposition of the electrolyte at the cathode, that is, the oxidation stability of the electrolyte was improved.^[120]

Although HCEs can induce the decomposition of salt anions to form inorganic-rich interfaces, their high viscosity limits their conductivity inside the bulk electrolyte. In addition, owing to the weak reduction stability of carbonate electrolytes, higher concentrations (>5 M) are required to achieve the high-concentration effect compared to ether electrolytes while most of the cost of electrolytes comes from the salt,^[125] hindering the commercialization of high concentration carbonate electrolytes. In light of this, partially replacing solvents with low-polarity inert solvents called diluents that weaken the interaction between Li^+ and the solvent to obtain LHCEs is believed to tackle the above problems.

Hydrofluoroether (HFE) is often chosen as the diluent, where the –F group near the ether bond reduces the electron density of the oxygen atom, weakening the ion–dipole interaction between Li^+ and HFE so that HFE is repelled to the outer layer of the Li^+ solvation structure.^[76] Therefore, diluents are immiscible with salts and have a minor influence on the original solvation structure. Chen et al. used bis(2,2,2-trifluoroethyl) ether (BTFE) as a diluent to prepare 1.2 M LiFSI in DMC/BTFE (1:2 by mol). DFT and ab initio molecular dynamics results indicate that the interaction between LiFSI and DMC is greater than that between LiFSI and BTFE, confirming the resultant formation of a salt anion-dominant solvation structure with the diluent remaining in the outer layer (Figure 6c).^[121] As verified by experiments, LHCEs not only retain the anion-dominated solvation structure ensuring the formation of a high-quality interface but also reduce the cost by lowering the concentration of salts needed.

Because of the retained solvation structure dominated by salt anions, LHCEs give an excellent battery performance. Fan et al. reported an LHCE of 1 M LiPF_6 in FEC:FEMC:HFE (2:6:2). Combining the advantages of LHCEs and the fluorination design, an F-rich SEI ($F\% \approx 45\%$) and CEI ($F\% \approx 60\%$) are formed at both electrodes (Figure 6d). Consequently, the NCM811 || Li cell cycles stably for 450 cycles at a rate of 0.5 C with a capacity retention of 90%. This also allows a LiCoPO_4 || Li cell to operate at a high voltage of 5.0 V, providing a high capacity retention of 93% after 1000 cycles at 1 C.^[52] Recently, a similar all-fluorinated LHCE of 1 M LiPF_6 in FEC:FEMC:1,1,2,3,3,3-hexafluoropropyl-2,2,2-trifluoroethyl ether (1:1:1) was reported by Zhang et al. and it exhibited excellent cycling stability over 1000 h in Li || Li cells and the capacity retention of the cell with $\text{LiNi}_{0.92}\text{Co}_{0.04}\text{Mn}_{0.04}\text{O}_2$ cathode was as high as 68% after 500 cycles at 5 V.^[126] Piao et al. prepared LiFSI/DMC/1,1,2,2-tetrafluoroethyl-2,2,3,3-tetrafluoropropyl ether (TTE) (1:1.5:1.5 by mol) with TTE as the diluent and strengthened the coordination between FSI^- with Li^+ by adding TTE as was proved by the shift of the $\text{Li}^+ - \text{FSI}^-$ peak in the Raman spectra, which is beneficial for the formation of

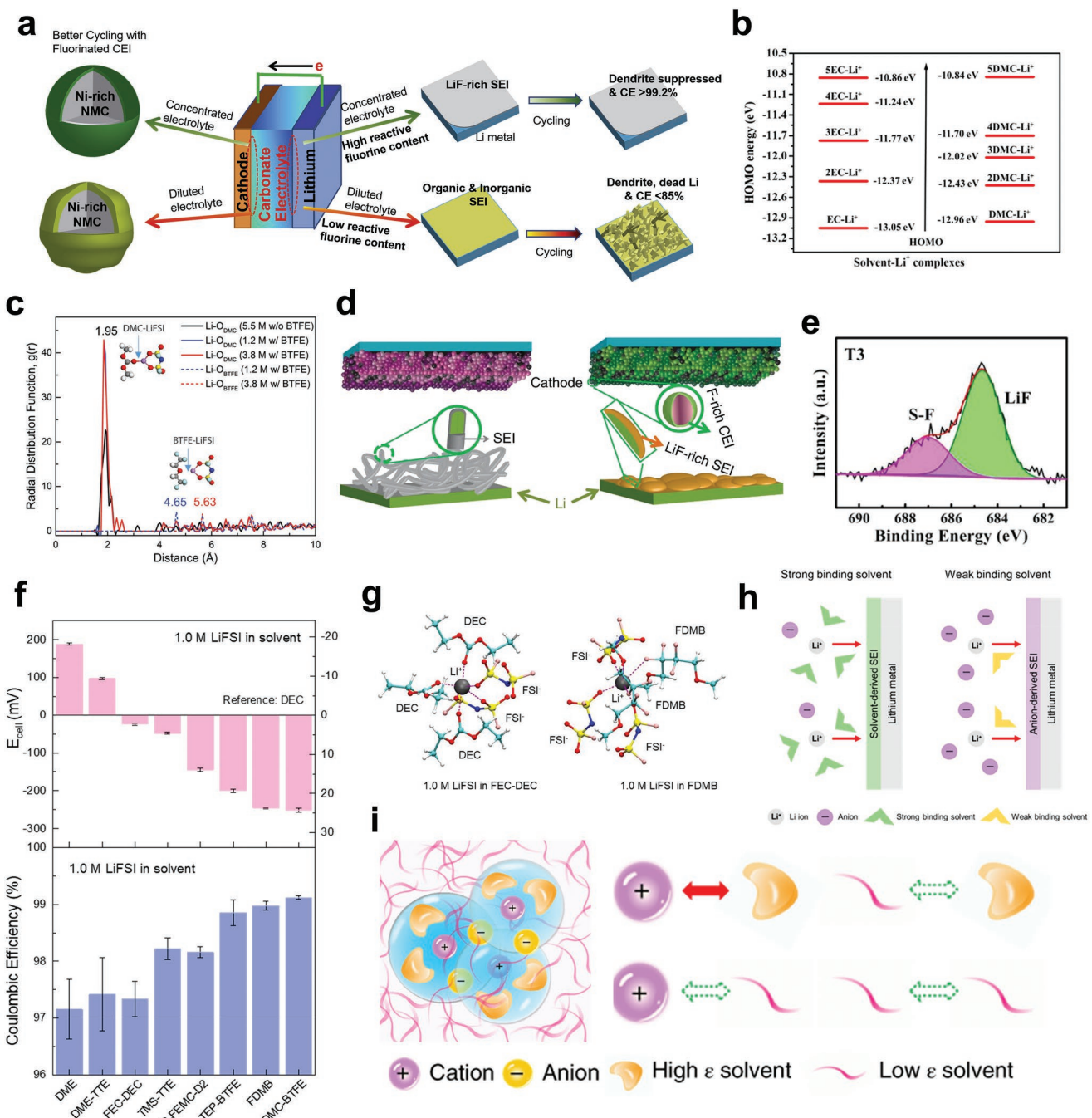


Figure 6. Characteristics and performance of modified carbonate electrolytes with a solvation structure dominated by salt anions. a) Schematic of the effect of a high concentration carbonate electrolyte on a Li metal anode and Ni-rich cathode. Reproduced with permission.^[119] Copyright 2018, Elsevier. b) The HOMO energy of n EC-Li⁺ and n DMC-Li⁺ ($1 \leq n \leq 5$) complexes with the change of Li⁺ concentration. Reproduced with permission.^[120] Copyright 2019, American Chemical Society. c) Radial distribution functions of Li-O_{DMC} and Li-O_{BTTF} pairs calculated from AIMD simulation trajectories at 30 °C, with insets showing the structures of DMC-LiFSI and BTFE-LiFSI solvent-salt pairs. Reproduced with permission.^[121] Copyright 2018, Wiley-VCH. d) Variation of SEI and CEI chemistries formed in a conventional carbonate electrolyte and LHCE. Reproduced with permission.^[52] Copyright 2018, Springer Nature. e) F 1s spectra of SEI after ten cycles in Li||Cu cells with an electrolyte of LiFSI/DMC/TTE (1:1.5:1.5 by mol). Reproduced with permission.^[122] Copyright 2020, Wiley-VCH. f) Solvation energy and Coulombic efficiencies of different electrolytes. g) Simulated solvation structures of different electrolytes. h) The relationship between solvent binding and structure, and the SEI formed in electrolytes. h) Reproduced with permission.^[123] Copyright 2021, American Chemical Society. i) Schematic of using a non-polar solvent to tame high concentration carbonate electrolytes and the affinities between solvents and ions. Reproduced with permission.^[124] Copyright 2019, Springer Nature.

an anion-induced F-rich interface (Figure 6e). Because of the high boiling point of TTE (92 °C), the high-temperature performance of the electrolyte was also improved. The capacity retention of NCM622||Li cells after 100 cycles with a cut-off voltage of 4.6 V reached 93.5% and 84.6% at room temperature and 60 °C, respectively.^[122] Further improvement of LHCEs was realized

of NCM622||Li cells after 100 cycles with a cut-off voltage of 4.6 V reached 93.5% and 84.6% at room temperature and 60 °C, respectively.^[122] Further improvement of LHCEs was realized

by Yu et al. who used a dual-salt system of LiFSI/LiDFOB in EC/EMC/BTFE. With the combined effect of the two salts, the LiF content in the interface was further increased, and for this reason, the Coulombic efficiency of the Li||Cu cell reached ~99%, and a $\text{LiCo}_{1/3}\text{Ni}_{1/3}\text{Mn}_{1/3}\text{O}_2\text{||Li}$ cell with a high loading of 3.8 mAh cm⁻² was stably cycled for 100 cycles under lean electrolyte conditions.^[61]

In addition to HCEs and LHCEs, weakly solvating electrolytes (WSEs) can also form a Li⁺ solvation structure dominated by salt anions only using weakly bound solvents that are miscible with salts, which leads to a stronger coordination of anions with Li⁺, resulting in an increase of the number of inorganic components in the interface.^[127,128] To verify the effectiveness of WSEs in improving battery performance, Kim et al. recently studied the relationship between the Coulombic efficiency and solvation energy of electrolytes, where 1 M LiFSI was dissolved in various solvents. As shown in Figure 6f, the Coulombic efficiency increases with decreasing interaction between the solvent and Li⁺. This is because weakly solvating solvents promote the participation of FSI⁻ in the solvation structure resulting in increased Li⁺-FSI⁻ coordination, which leads to increased decomposition of anions at the anode forming an anion-derived SEI rather than a solvent-derived one (Figure 6g,h).^[123]

A critical benefit produced by weakening the interaction between the Li⁺ and the solvent in a solvation structure dominated by salt anions involves the reduction of the Li⁺ de-solvation energy barrier, which is desirable for low-temperature applications. It has been reported that after the introduction of a non-polar diluent (tetrafluoro-1-(2,2,2-trifluoroethoxy)ethane (D2) (Figure 6i), the de-solvation process is significantly improved as proven by calculations of the Li⁺ solvation/de-solvation energy in different electrolytes. As a result, an electrolyte diluted by D2 can even work at an extremely low temperature of -80 °C, and a $\text{LiNi}_{0.8}\text{Co}_{0.15}\text{Al}_{0.05}\text{O}_2\text{||Li}$ battery exhibited good cycling stability at -20 °C, maintaining a high capacity of 150 mAh g⁻¹ after 450 cycles. In comparison, a battery with a baseline dilute electrolyte only provided a capacity of 35 mAh g⁻¹ after 100 cycles followed by a rapid capacity decay.^[124]

To conclude, a solvation structure of Li⁺ dominated by salt anions produces many different improvements. The inorganic-rich interfaces derived from salt anions greatly improve battery performance, and because of the lower HOMO values, oxidation stability is also improved. In addition, the de-solvation process of Li⁺ is also improved because of the weakened interaction between Li⁺ and the solvent. However, although an anion-dominant solvation structure helps improve interface kinetics such as forming an inorganic-rich SEI and reducing the de-solvation barrier, it sacrifices the ionic conductivity of Li⁺ in bulk electrolytes due to less dissociation of cations and anions. It is therefore important to strike a balance between the kinetics at the interface and in the bulk.

3.4. Modified Carbonate Electrolytes with a Solvation Structure Dominated by Fluorinated Carbonates

The fluorination of carbonate solvents is another emerging approach to develop advanced carbonate electrolytes with sol-

vation structures dominated by carbonates. By careful regulation of the solvation structure of Li⁺, the performance of such electrolytes can far exceed those of conventional EC-based electrolytes which also have solvation structures dominated by carbonates.

Among the various fluorinated carbonates, FEC is the most attractive due to its good film-forming ability caused by a low LUMO energy level, which enables it to preferentially decompose at the anode to form an F-rich SEI. To confirm the efficacy of FEC in improving battery performance, Markevich et al. replaced EC with FEC to prepare 1 M LiPF₆ in FEC/DMC. Li||Li cells with this electrolyte cycled stably for 3500 h at a current density of 2 mA cm⁻² and a capacity of 3.3 mAh cm⁻², demonstrating the effectiveness of FEC in improving battery performance (Figure 7a).^[51] Archer's group used FEC and diglyme (G2) to further enrich the F content in the SEI. Here, G2 acted as a "cleaning agent" to solubilize the unwanted carbonaceous compounds while preserving the insoluble LiF in the SEI (Figure 7b,c), enabling higher reversibility, longer cycle life, and improved morphology of the lithium metal anode.^[91] Di-fluoro ethylene carbonate (DFEC), synthesized by further fluorination of FEC, is another emerging film-forming agent. As shown by DFT calculation results, the LUMO energy level of DFEC is as low as -0.66 eV, much lower than EC (-0.30 eV) and FEC (-0.39 eV) (Figure 7d), and this is favorable for the formation of a LiF-rich SEI at the anode.^[55] The incorporation of DFEC not only helps form a stable SEI at the anode to regulate the plating/stripping of Li⁺ but also improves the oxidation stability of the electrolyte against the cathode. As shown in Figure 7e, a NCM622||Li cell with DFEC has a very low leakage current and maintains 82% of its initial capacity after 400 cycles.^[129] It has also been reported that DFEC can suppress crosstalk in NCM||Li cells using FEC as a single solvent, indicating the combined effect of DFEC and FEC.^[54] Some all-fluorinated systems also show excellent performance. Using 1 M LiPF₆ in a methyl 3,3,3-trifluoropionate (MTFP)/FEC (9:1) electrolyte, a NCM811||Li cell had a high capacity retention of 80% after 250 cycles at a cut-off voltage of 4.5 V.^[130] Recently, Cheng's group reported an all-fluorinated ultra-high voltage resistant electrolyte composed of FEC and bis(2,2,2-trifluoroethyl) carbonate (BTC) as the solvents for LMBs, where BTC was obtained by the addition of F atoms to DEC. Because of the fluorination of the solvents, NCM811||Li cells had high capacity retention of 85.7% after 100 cycles with a cut-off voltage of 4.8 V (Figure 7f).^[131]

Except for the energy levels of the individual components, the as-formed solvation structure of Li⁺ also significantly influences the preference of components participating in the interface formation. Su et al. showed that despite the LUMO of DFEC being lower than that of FEC, FEC is more desirable than DFEC for FEMC-based electrolytes as shown by the better cycling stability of a FEC/FEMC electrolyte than a DFEC/FEMC electrolyte. This is because the order of Li⁺ solvating power is FEC > FEMC > DFEC, which means that the Li⁺ solvation structure is occupied by FEC in the FEC/FEMC electrolyte while FEMC is more dominant in the solvation structure of DFEC/FEMC electrolyte. Therefore, FEMC is more likely to be reduced in the DFEC/FEMC electrolyte to form detrimental products on the anode, while FEC is preferentially reduced in

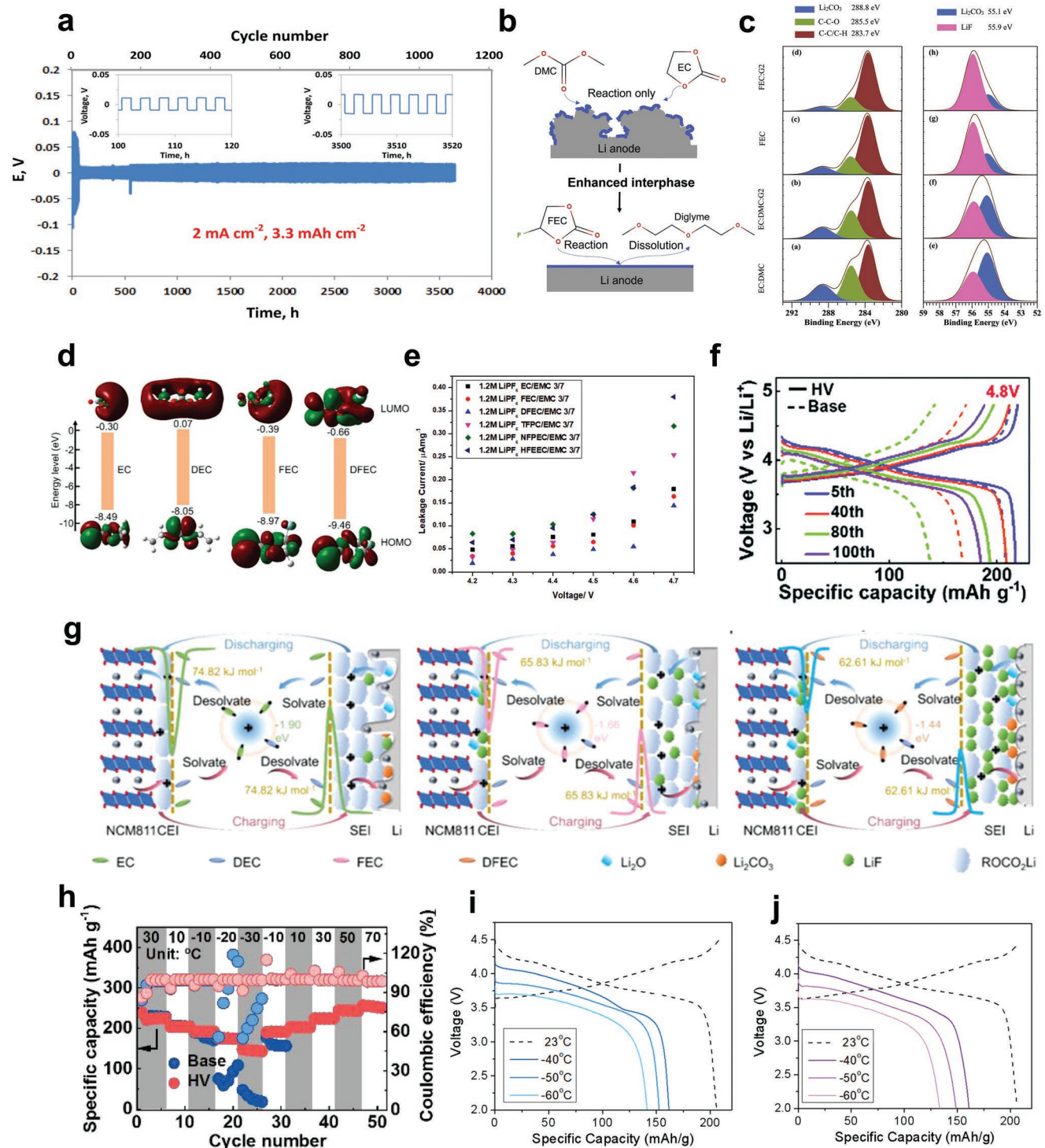


Figure 7. Characteristics and performance of carbonate electrolytes with a solvation structure dominated by fluorinated carbonates. a) Galvanostatic cycling performance of Li||Li cells cycled with 1 M LiPF₆ in FEC/DMC at a current density of 2 mA cm⁻². Reproduced with permission.^[51] Copyright 2017, American Chemical Society. b) Schematic of the reaction-dissolution strategy to enhance the reversibility of Li anode. c) C 1s and Li 1s spectra of SEI formed on Li in different electrolytes. b,c) Reproduced with permission.^[91] Copyright 2022, Elsevier. d) Schematic of the LUMO/HOMO energies of EC, DEC, FEC, and DFEC. Reproduced with permission.^[55] Copyright 2021, Wiley-VCH. e) Variation of the static leakage current as a function of potential for different cyclic carbonate-based electrolytes in NMC622||Li cells. Reproduced with permission.^[129] Copyright 2019, Elsevier. f) Charge–discharge curves of NCM811||Li cells using different electrolytes at 0.5 C with a cut-off voltage of 4.8 V. Reproduced with permission.^[131] Copyright 2022, Royal Society of Chemistry. g) Schematic of the dynamic evolution of Li⁺ solvation sheath during charging/discharging in different electrolytes. Reproduced with permission.^[55] Copyright 2021, Wiley-VCH. h) Electrochemical performance of NCM811||Li cells using different electrolytes at temperatures from -30 to 70 °C with a cut-off voltage of 4.7 V. Reproduced with permission.^[131] Copyright 2022, Royal Society of Chemistry. Voltage profiles of NMC 811||Li cells in i) 1 M LiPF₆ MP/FEC and j) 1 M LiPF₆ MTFP/FEC at low temperatures. Reproduced with permission.^[130] Copyright 2020, American Chemical Society.

the FEC/FEMC electrolyte to retard the unfavorable reduction of FEMC.^[53] Later work showed that adding FEC to the DFEC/FEMC electrolyte significantly improved the performance, which agrees with previous conclusions.^[56] Therefore, in addition to the thermodynamic properties of the individual components, the solvation structure of Li⁺ should be carefully considered in understanding the formation of the interface.

Furthermore, because of the weak interaction between a fluorinated carbonate and Li⁺, fluorinated carbonates also bring advantages in terms of improving the de-solvation process, thereby improving the low-temperature performance. Wang et al. compared the ion-dipole interaction strengths of carbonate electrolytes with different degrees of fluorination and found that the ion-dipole interaction strength of a DFEC-based electrolytes is as low as 1.44 eV, much lower than that of EC-based (1.90 eV) and FEC-based (1.66 eV) electrolytes (Figure 7g). As a result, a NCM811||Li cell using a DFEC-based electrolyte maintained 51% of its room temperature capacity at -30 °C, while the capacity of a 1 M LiPF₆ EC/DEC battery was close to zero at 0 °C.^[55] Similarly, Xiao et al. calculated the binding energy between Li⁺ and solvents before and after fluorination and the results are in excellent agreement with previous studies. Because of the weakened interaction between solvents and Li⁺, the activation energy for the de-solvation process is decreased by using fluorinated carbonates, and NCM811||Li cells had a high reversible capacity of 143.5 mAh g⁻¹ even at a temperature as low as -30 °C (Figure 7h).^[131] Holoubek et al. used methyl propionate (MP) and fluorinated solvents including MTFP and FEC to develop ultra-low temperature electrolytes and NCM811||Li cells with these electrolytes had an excellent low-temperature performance delivering ≈80%, 73–75%, and 65–70% of room temperature capacity at -40, -50, and -60 °C, respectively (Figure 7i,j).^[130]

In conclusion, a number of fluorinated carbonate electrolytes have been proposed to regulate the solvation structure and improve the performance of LMBs. Their most significant role is to help form F-rich interfaces at both electrodes and improve oxidation stability due to the lowered HOMO energy level. In addition to helping form F-rich interfaces, fluorination also accelerates the de-solvation process because of the reduced Li⁺ solvating power, which helps improve the low-temperature cycling stability. However, fluorination greatly increases the cost and is environmentally unfriendly and future research must consider these factors.

3.5. Discussion on the Combined Effect of “Cocktail Strategy”

To improve the performance of the electrolyte in multiple aspects, some of the above individual strategies with unique advantages can be used together and it often brings a combined effect (Figure 8a).

As reported, when additives are introduced to the solvation structure that is rich in fluorinated carbonates, the overall performance could be further improved. Zhang's group added LiNO₃ into an FEC-based electrolyte, and both LiNO₃ and FEC contributed to the formation of SEI. As a result, a uniform and rapid Li⁺ diffusion in the SEI was achieved due to its abundance in LiF and LiN_xO_y, so the electrolyte delivered a much-prolonged

cycle life and high Coulombic efficiency (Figure 8b).^[109] Similar results were obtained by Wang's group that LiF, LiN_xO_y, and Li₃N were enriched in the SEI in the electrolyte with LiNO₃ and FEC (Figure 8c).^[42] Wang et al. further analyzed the individual and a combined effect of LiNO₃ and FEC. The morphology of the lithium deposits in the electrolyte with FEC and both FEC/LiNO₃ was different. As shown in Figure 8d, it presented a non-dendric morphology after using fluorinated solvents, but obvious voids between deposits were observed. With the further addition of LiNO₃, the whole surface was flatly covered with few dead Li and by-products. This is consistent with the results of Coulombic efficiency where the electrolyte with FEC/LiNO₃ showed the highest Coulombic efficiency of 98.6%, much higher than that only with FEC (96.3%) in Figure 8e.^[108] LiDFOB as another effective additive can also bring a positive impact. When a small amount of LiDFOB (1 wt%) is added to an FEC-containing electrolyte, they can reduce the consumption rate of each other and the electrolyte as evidenced by ¹⁹F quantitative NMR results. Excellent retention of LiPF₆ (99.4%), FEC (97.8%), and LiDFOB (81.0%) was achieved after ten cycles in the electrolyte with FEC/LiDFOB (Figure 8f), making those components more long-lasting during cycling. Due to their improved sustainability, the Li||Cu and NCM811||Li cells exhibited much more stable cycling compared to the baseline electrolyte and that only with FEC (Figure 8g), confirming the combined effect of FEC and LiDFOB.^[60]

The introduction of additives to the solvation structure dominated by salt anions also delivers a combined effect. Zhang's group used BTFE as the diluent to obtain a LHCE and the cycling performance of the Li||Cu cells and Li||Li cells was significantly improved with long cycling life, low polarization voltage, and high Coulombic efficiency (Figure 8h), indicating the effectiveness of the solvation structure dominated by salt anions. The addition of 0.15 M LiDFOB to this LHCE further improved the performance of both electrodes arising from its critical role in helping form elastic and stable oligomer-rich SEI. Therefore, in this LiDFOB-modified LHCE electrolyte, the unique advantages of LHCE and additives were displayed together.^[61]

In addition, different kinds of additives can make the most of their respective advantages when they are used together. For example, when PFN and LiDFOB were used simultaneously, stable interfaces were formed on both electrodes due to the excellent film-forming capability of LiDFOB with low LUMO and high HOMO energy levels, while PFN played a role in suppressing HF generation by catching PF₅ and HF.^[27]

Collectively, some of the above four strategies do bring a combined effect when they are used together, mostly when additives are introduced to modified solvation structures. However, it does not necessarily mean any random combination has a positive effect since the interaction between original and newly introduced components is uncertain and its change may result in totally different scenarios.

4. Summary and Outlook

With the increasing demand for high-energy-density batteries, lithium metal anode and high-voltage cathode have attracted

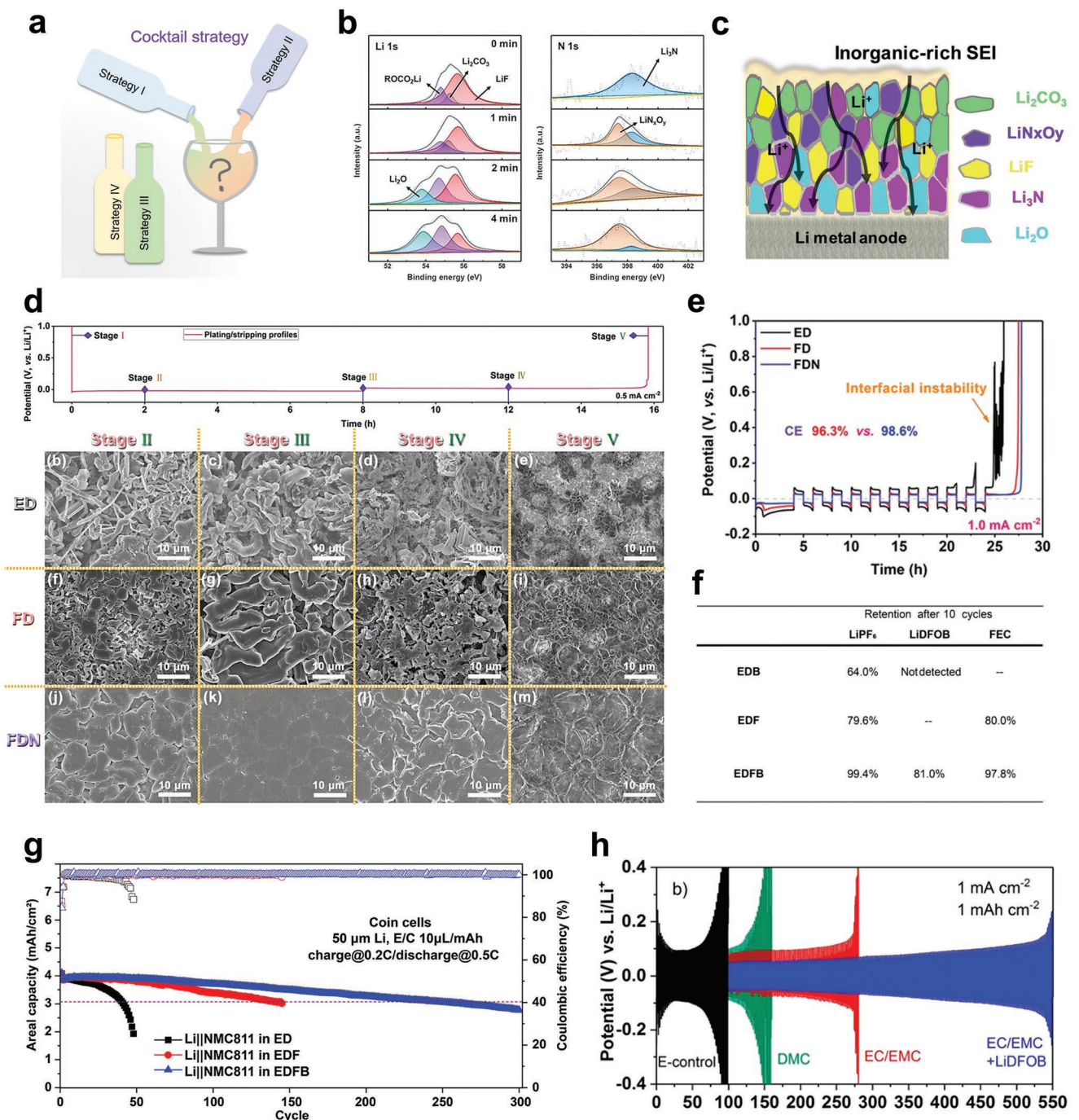


Figure 8. Characteristics and performance of carbonate electrolytes modified by “cocktail strategy.” a) Schematic of “cocktail strategy.” b) In-depth X-ray photoelectron spectroscopy spectra of SEI formed on lithium after 100 cycles in the electrolyte with FEC/LiNO₃. Reproduced with permission.^[109] Copyright 2018, Wiley-VCH. c) Schematic of the structure of the SEI formed in the electrolyte with FEC/LiNO₃. Reproduced with permission.^[42] Copyright 2020, Wiley-VCH. d) SEM images of Li plating onto Cu substrate in different electrolytes. e,f) Reproduced with permission.^[108] Copyright 2021, Wiley-VCH. f) Summary of F-containing components retention in different electrolytes after ten cycles. g,f,g) Reproduced with permission.^[60] Copyright 2022, American Chemical Society. h) Galvanostatic cycling voltage profiles for Li||Li cells with different electrolytes. Reproduced with permission.^[61] Copyright 2018, American Chemical Society.

much attention. However, commercial conventional carbonate electrolytes fail to sustain stable operation with these electrodes, which necessitates the revolution of interface chemistry in car-

bonate electrolytes. In recent years, significant progress has been made in exploring basic knowledge and improving the performance of carbonate electrolytes for high-voltage LMBs.

In this review, we have comprehensively reviewed the critical effects of four types of carbonate electrolytes with modified solvation structures on Li^+ behavior and battery performance. The performance of carbonate electrolytes with different solvation structures in terms of cost, oxidation stability, film-forming ability, ionic mobility, de-solvation kinetics, and thermal stability are summarized below (Figure 9).

The use of additives is the most cost-effective way of improving carbonate electrolytes since only a small amount is required. Using multi-functional additives can improve interfaces on both electrodes, and by incorporating special additives that have a strong interaction with Li^+ or special anions like Br^- , the de-solvation process can be improved. In addition, many additives have been proposed with functions such as scavenging HF, which improves the thermal stability of LiPF_6 -containing carbonate electrolytes.

As a special case of additive regulation strategies, the addition of NO_3^- with a high DN causes the solvation structure to be dominated by anions other than solvents, which improves the de-solvation process but lowers the Li^+ mobility. The salt anions are also repelled from Li^+ , so LiPF_6 decomposition is suppressed, improving the thermal stability of the electrolytes. In addition, NO_3^- with a low LUMO level preferentially decomposes upon contact with the Li metal anode to form a highly

conductive Li_3N -rich interface. However, NO_3^- has poor oxidation resistance in the presence of high-voltage cathodes, which decreases its effect at high voltages.

Constructing a solvation structure dominated by salt anions is another effective way to improve various properties of carbonate electrolytes. This solvation structure can be obtained in two ways. One is to increase the salt concentration and the other is to decrease the solvating power of a solvent. In electrolytes with this solvation structure, salt anions play a dominant role in forming interfaces and remaining stable against electrodes. Thanks to the superior film-forming ability and oxidation stability of anions compared to solvents, the assembled battery shows great interfacial stability. In most cases, LiTFSI and LiFSI salts are used and the content of thermally unstable solvents is reduced, so the thermal stability of carbonate electrolytes is improved. Furthermore, due to the modified solvation structure with weakened Li^+ -solvent interaction and increased Li^+ -anion interaction, the de-solvation process is accelerated while the mobility of Li^+ is reduced, which requires to balance the two effects.

Fluorination, which lowers the HOMO and LUMO energy levels of the molecules, is also widely used for improving carbonate electrolytes. Lower HOMO and LUMO energy levels mean its good stability against cathodes and easy reduction of the

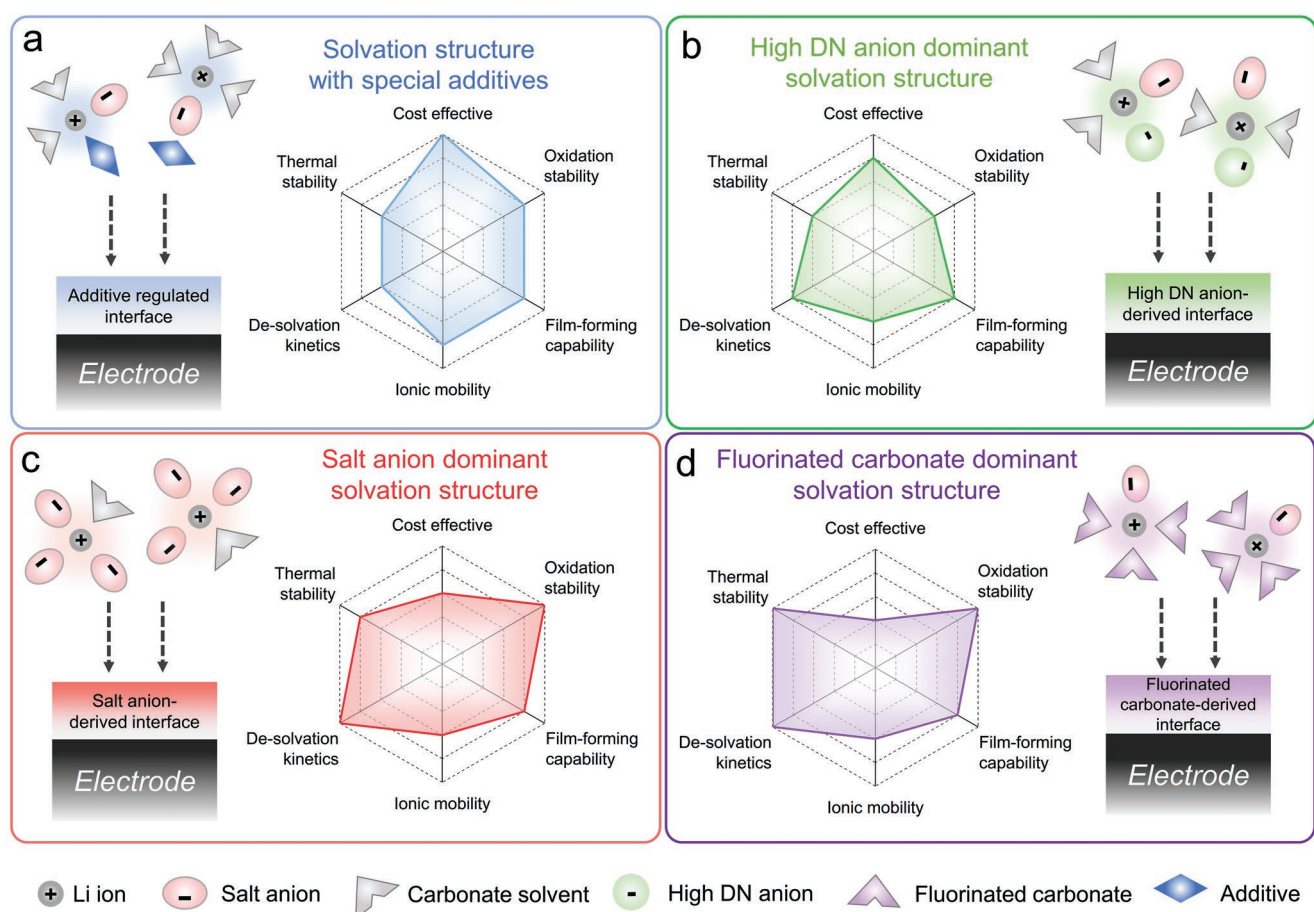


Figure 9. Schematic of the solvation structures and summary of the performance metrics of LMBs in four types of modified carbonate electrolytes with solvation structures a) with special additives, b) dominated by high DN anions, c) dominated by salt anions, and d) dominated by fluorinated carbonates.

molecule at the anode while the formation of an F-rich interface is highly desirable. Unlike carbonate electrolytes with a solvation structure dominated by salt anions, electrolytes with fluorination hardly contain electrochemically unstable components thereby increasing the oxidation stability of the electrolytes. Another effect of fluorination is the weakening of Li^+ solvating power. Weakened interaction between fluorinated carbonates and Li^+ is favorable for the de-solvation of the solvation structure, improving the low-temperature performance. Moreover, the inherent non-flammability of fluorinated components ensures the safety of the electrolytes at high temperatures. However, the biggest drawback is its high cost and harmful effect on the environment.

Despite many encouraging results having been reported, a series of scientific and technical problems regarding the Li^+ solvation structure in carbonate electrolytes for LMBs remains to be solved (Figure 10).

1) A lack of understanding the relationship between the composition/physical properties of components and the Li^+ solvation structure. Although some theoretical calculations and characterization methods have been developed, there is still a long way to go to accurately predict and design the Li^+ solvation structure in carbonate electrolytes. Therefore, more effort should be made in exploring advanced solvation structure characterization methods and studying the connections between the solvation structure and the composition/physical properties of components.

- 2) A lack of understanding the interface formed by different solvation structures. Most studies use X-ray photoelectron spectroscopy to characterize interfaces, whose resolution is not sufficient to give information at the atomic level, which calls for high-resolution characterization methods. Although cryogenic transmission electron microscope is still at the preliminary stage, it may be a potent tool for obtaining a deep understanding of the interfaces formed by various solvation structures in carbonate electrolytes.
- 3) Rational design of solvation structures. In the process of developing high-performance electrolytes, we often ignore the cost and impact on the environment, pursuing only good performance. Although fluorination significantly improves performance, it is expensive and environment-unfriendly, and for this reason, more attention is needed before possible commercialization. Research must focus on novel solvation structures taking cost and environmental issues into account.
- 4) Evaluation of the effectiveness of solvation structures in practical conditions. The practicality of electrolytes must be brought to the forefront. The effects of different solvation structures have been mostly evaluated in coin cells with a sufficient lithium supply, sufficient electrolyte, and low loading. To better assess these effects, a strict and standard protocol for testing should be established. In addition, more effort is needed to develop electrolytes operating in a wide temperature range.
- 5) Combination of experiments with machine learning to predict the effects of specific solvation structures. The

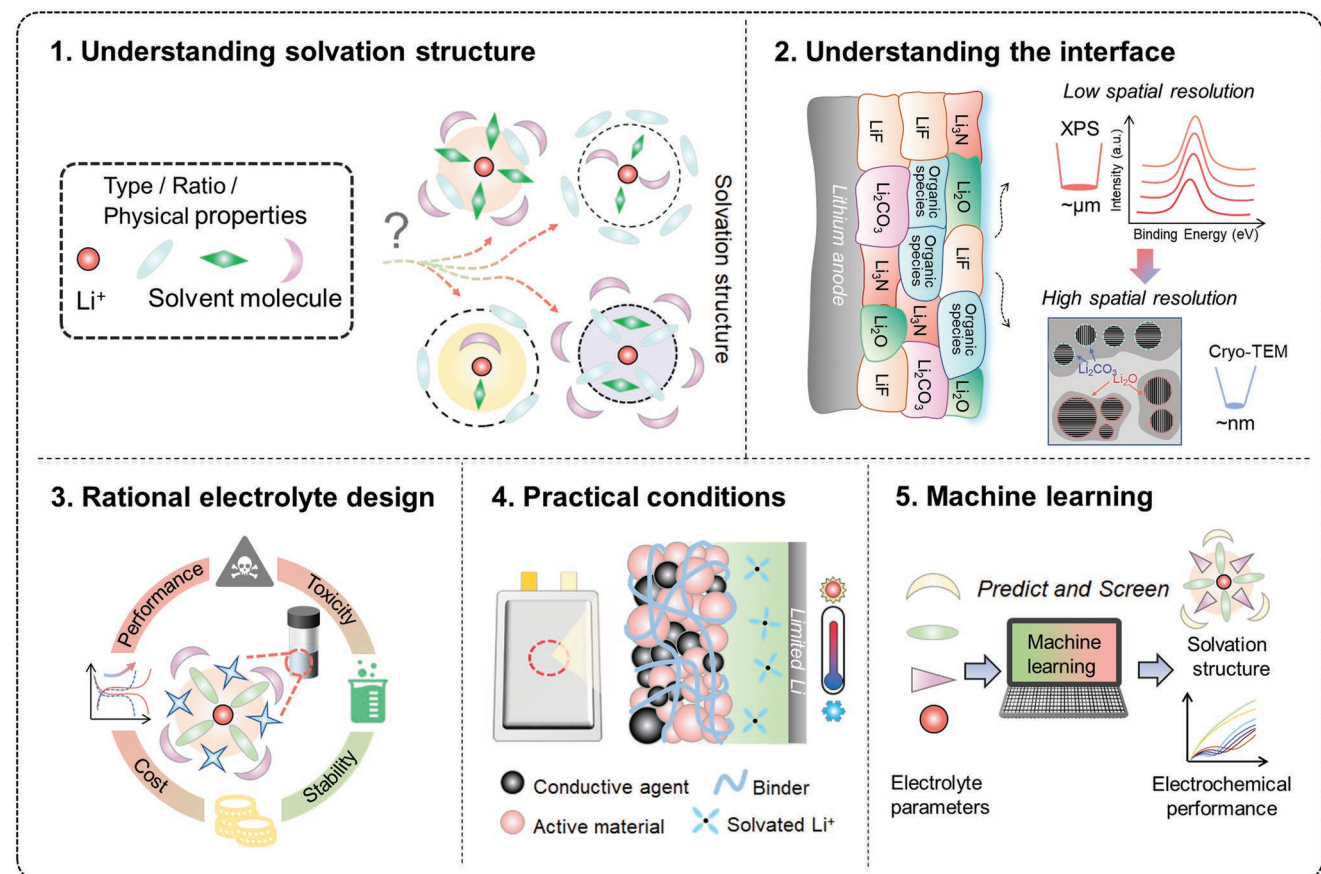


Figure 10. Outlook for developing advanced carbonate electrolytes.

mainstream research method so far has been trial and error, which costs a lot of money and manpower. Artificial intelligence and machine learning can assist researchers in effectively analyzing the huge amount of data from previous research and provide predictions of the performance of new solvation structures. This would help with preliminary screening to avoid repetitive experimental work.

To summarize, based on the results achieved previously and discussions mentioned above, it is reasonable to say that there are currently no “one for all” carbonate electrolytes that perform well in all aspects. Therefore, it is important to design the solvation structure of carbonate electrolytes for specific uses. While it is critical to take advantage of different solvation structures, the investigation of new carbonate electrolytes with a novel solvation structure is highly encouraged. Although many scientific and technological challenges need to be solved, we hope this review provides a guide to help fundamentally investigate the science behind Li⁺ solvation structure, Li⁺ behavior, and battery performance in carbonate electrolytes and rationally design acceptable carbonate electrolytes for practical LMBs.

Acknowledgements

The authors appreciate the support from the National Key Research and Development Program of China (2021YFB2500200 and 2019YFA0705700), the National Natural Science Foundation of China (No. 52072205), Joint Funds of the National Natural Science Foundation of China (U21A20174), the Overseas Research Cooperation Fund of Tsinghua Shenzhen International Graduate School, and the Shenzhen Geim Graphene Center.

Conflict of Interest

The authors declare no conflict of interest.

Keywords

carbonate electrolytes, Li⁺ behaviors, lithium metal batteries, solvation structures

Received: July 1, 2022

Revised: August 17, 2022

Published online: February 23, 2023

- [1] S. Yuan, T. Kong, Y. Zhang, P. Dong, Y. Zhang, X. Dong, Y. Wang, Y. Xia, *Angew. Chem., Int. Ed.* **2021**, *60*, 25624.
- [2] G. G. Eshetu, H. Zhang, X. Judez, H. Adenusi, M. Armand, S. Passerini, E. Figgemeier, *Nat. Commun.* **2021**, *12*, 5459.
- [3] S. Mao, Q. Wu, F. Ma, Y. Zhao, T. Wu, Y. Lu, *Chem. Commun.* **2021**, *57*, 840.
- [4] M. Shulan, W. Qian, W. Zhuoya, L. Yingying, *Energy Storage Sci. Technol.* **2020**, *9*, 538.
- [5] Y. Tian, G. Zeng, A. Rutt, T. Shi, H. Kim, J. Wang, J. Koettgen, Y. Sun, B. Ouyang, T. Chen, Z. Lun, Z. Rong, K. Persson, G. Ceder, *Chem. Rev.* **2021**, *121*, 1623.
- [6] X. Fan, C. Wang, *Chem. Soc. Rev.* **2021**, *50*, 10486.
- [7] Q. Zhao, S. Stalin, L. A. Archer, *Joule* **2021**, *5*, 1119.

- [8] X. R. Chen, B. C. Zhao, C. Yan, Q. Zhang, *Adv. Mater.* **2021**, *33*, 2004128.
- [9] Y. Jie, X. Ren, R. Cao, W. Cai, S. Jiao, *Adv. Funct. Mater.* **2020**, *30*, 1910777.
- [10] B. Liu, J.-G. Zhang, W. Xu, *Joule* **2018**, *2*, 833.
- [11] W. Ren, Y. Zheng, Z. Cui, Y. Tao, B. Li, W. Wang, *Energy Storage Mater.* **2021**, *35*, 157.
- [12] X. Zhu, K. Wang, Y. Xu, G. Zhang, S. Li, C. Li, X. Zhang, X. Sun, X. Ge, Y. Ma, *Energy Storage Mater.* **2021**, *36*, 291.
- [13] X. Zheng, L. Huang, X. Ye, J. Zhang, F. Min, W. Luo, Y. Huang, *Chem* **2021**, *7*, 2312.
- [14] N. Zhang, T. Deng, S. Zhang, C. Wang, L. Chen, C. Wang, X. Fan, *Adv. Mater.* **2022**, *34*, 2107899.
- [15] K. Qin, K. Holguin, M. Mohammadiroobari, J. Huang, E. Y. S. Kim, R. Hall, C. Luo, *Adv. Funct. Mater.* **2021**, *31*, 2009694.
- [16] Y. Gao, X. Du, Z. Hou, X. Shen, Y.-W. Mai, J.-M. Tarascon, B. Zhang, *Joule* **2021**, *5*, 1860.
- [17] X. Ren, L. Zou, X. Cao, M. H. Engelhard, W. Liu, S. D. Burton, H. Lee, C. Niu, B. E. Matthews, Z. Zhu, C. Wang, B. W. Arey, J. Xiao, J. Liu, J. G. Zhang, W. Xu, *Joule* **2019**, *3*, 1662.
- [18] X. Ren, X. Zhang, Z. Shadike, L. Zou, H. Jia, X. Cao, M. H. Engelhard, B. E. Matthews, C. Wang, B. W. Arey, X. Q. Yang, J. Liu, J. G. Zhang, W. Xu, *Adv. Mater.* **2020**, *32*, 2004898.
- [19] X. Cao, P. Gao, X. Ren, L. Zou, M. H. Engelhard, B. E. Matthews, J. Hu, C. Niu, D. Liu, B. W. Arey, C. Wang, J. Xiao, J. Liu, W. Xu, J. G. Zhang, *Proc. Natl. Acad. Sci. U. S. A.* **2021**, *118*, e202035718.
- [20] Y. Chen, Z. Yu, P. Rudnicki, H. Gong, Z. Huang, S. C. Kim, J. C. Lai, X. Kong, J. Qin, Y. Cui, Z. Bao, *J. Am. Chem. Soc.* **2021**, *143*, 18703.
- [21] R. Xu, J. F. Ding, X. X. Ma, C. Yan, Y. X. Yao, J. Q. Huang, *Adv. Mater.* **2021**, *33*, 2105962.
- [22] J. Holoubek, K. Kim, Y. Yin, Z. Wu, H. Liu, M. Li, A. Chen, H. Gao, G. Cai, T. A. Pascal, P. Liu, Z. Chen, *Energy Environ. Sci.* **2022**, *15*, 1647.
- [23] D. Luo, M. Li, Y. Zheng, Q. Ma, R. Gao, Z. Zhang, H. Dou, G. Wen, L. Shui, A. Yu, X. Wang, Z. Chen, *Adv. Sci.* **2021**, *8*, 2101051.
- [24] J. Langdon, R. Sim, A. Manthiram, *ACS Energy Lett.* **2022**, *7*, 2634.
- [25] J. G. Zhang, W. Xu, J. Xiao, X. Cao, J. Liu, *Chem. Rev.* **2020**, *120*, 13312.
- [26] J. G. Han, K. Kim, Y. Lee, N. S. Choi, *Adv. Mater.* **2019**, *31*, 1804822.
- [27] L. Zhang, F. Min, Y. Luo, G. Dang, H. Gu, Q. Dong, M. Zhang, L. Sheng, Y. Shen, L. Chen, J. Xie, *Nano Energy* **2022**, *96*, 107122.
- [28] C. L. Campion, W. Li, B. L. Lucht, *J. Electrochem. Soc.* **2005**, *152*, A2327.
- [29] X. Zheng, L. Huang, W. Luo, H. Wang, Y. Dai, X. Liu, Z. Wang, H. Zheng, Y. Huang, *ACS Energy Lett.* **2021**, *6*, 2054.
- [30] H. Wu, H. Jia, C. Wang, J. G. Zhang, W. Xu, *Adv. Energy Mater.* **2020**, *11*, 2003092.
- [31] X. B. Cheng, R. Zhang, C. Z. Zhao, F. Wei, J. G. Zhang, Q. Zhang, *Adv. Sci.* **2016**, *3*, 1500213.
- [32] Y. Feng, L. M. Zhou, H. Ma, Z. H. Wu, Q. Zhao, H. X. Li, K. Zhang, J. Chen, *Energy Environ. Sci.* **2022**, *15*, 1711.
- [33] S. E. Sloop, J. B. Kerr, K. Kinoshita, *J. Power Sources* **2003**, *119–121*, 330.
- [34] L. Chen, H. Wu, X. Ai, Y. Cao, Z. Chen, *Battery Energy* **2022**, *1*, 20210006.
- [35] J. Holoubek, H. Liu, Z. Wu, Y. Yin, X. Xing, G. Cai, S. Yu, H. Zhou, T. A. Pascal, Z. Chen, P. Liu, *Nat. Energy* **2021**, *6*, 303.
- [36] L. Dong, Y. Liu, K. Wen, D. Chen, D. Rao, J. Liu, B. Yuan, Y. Dong, Z. Wu, Y. Liang, M. Yang, J. Ma, C. Yang, C. Xia, B. Xia, J. Han, G. Wang, Z. Guo, W. He, *Adv. Sci.* **2022**, *9*, 2104699.
- [37] S. Lin, H. Hua, Z. Li, J. Zhao, *ACS Appl. Mater. Interfaces* **2020**, *12*, 33710.
- [38] J. Alvarado, M. A. Schroeder, T. P. Pollard, X. Wang, J. Z. Lee, M. Zhang, T. Wynn, M. Ding, O. Borodin, Y. S. Meng, K. Xu, *Energy Environ. Sci.* **2019**, *12*, 780.

- [39] S. Jiao, X. Ren, R. Cao, M. H. Engelhard, Y. Liu, D. Hu, D. Mei, J. Zheng, W. Zhao, Q. Li, N. Liu, B. D. Adams, C. Ma, J. Liu, J.-G. Zhang, W. Xu, *Nat. Energy* **2018**, *3*, 739.
- [40] M. Zhou, P. Bai, X. Ji, J. Yang, C. Wang, Y. Xu, *Adv. Mater.* **2021**, *33*, 2003741.
- [41] K. Xu, *Chem. Rev.* **2014**, *114*, 11503.
- [42] S. Liu, X. Ji, N. Piao, J. Chen, N. Eidson, J. Xu, P. Wang, L. Chen, J. Zhang, T. Deng, S. Hou, T. Jin, H. Wan, J. Li, J. Tu, C. Wang, *Angew. Chem., Int. Ed.* **2021**, *60*, 3661.
- [43] M. Baek, H. Shin, K. Char, J. W. Choi, *Adv. Mater.* **2020**, *32*, 2005022.
- [44] Y. Jie, X. Liu, Z. Lei, S. Wang, Y. Chen, F. Huang, R. Cao, G. Zhang, S. Jiao, *Angew. Chem., Int. Ed.* **2020**, *59*, 3505.
- [45] K. Xu, A. von Wald Cresce, *J. Mater. Res.* **2012**, *27*, 2327.
- [46] X. Dong, Z. Guo, Z. Guo, Y. Wang, Y. Xia, *Joule* **2018**, *2*, 902.
- [47] Z. Geng, J. Lu, Q. Li, J. Qiu, Y. Wang, J. Peng, J. Huang, W. Li, X. Yu, H. Li, *Energy Storage Mater.* **2019**, *23*, 646.
- [48] N. Piao, S. Liu, B. Zhang, X. Ji, X. Fan, L. Wang, P.-F. Wang, T. Jin, S.-C. Liou, H. Yang, J. Jiang, K. Xu, M. A. Schroeder, X. He, C. Wang, *ACS Energy Lett.* **2021**, *6*, 1839.
- [49] B. Han, Z. Zhang, Y. Zou, K. Xu, G. Xu, H. Wang, H. Meng, Y. Deng, J. Li, M. Gu, *Adv. Mater.* **2021**, *33*, 2100404.
- [50] Z. Chang, Y. Qiao, H. Yang, H. Deng, X. Zhu, P. He, H. Zhou, *Energy Environ. Sci.* **2020**, *13*, 4122.
- [51] E. Markevich, G. Salitra, F. Chesneau, M. Schmidt, D. Aurbach, *ACS Energy Lett.* **2017**, *2*, 1321.
- [52] X. Fan, L. Chen, O. Borodin, X. Ji, J. Chen, S. Hou, T. Deng, J. Zheng, C. Yang, S. C. Liou, K. Amine, K. Xu, C. Wang, *Nat. Nanotechnol.* **2018**, *13*, 715.
- [53] C.-C. Su, M. He, R. Amine, T. Rojas, L. Cheng, A. T. Ngo, K. Amine, *Energy Environ. Sci.* **2019**, *12*, 1249.
- [54] D. Aurbach, E. Markevich, G. Salitra, *J. Am. Chem. Soc.* **2021**, *143*, 21161.
- [55] Z. Wang, Z. Sun, Y. Shi, F. Qi, X. Gao, H. Yang, H. M. Cheng, F. Li, *Adv. Energy Mater.* **2021**, *11*, 2100935.
- [56] C.-C. Su, M. He, M. Cai, J. Shi, R. Amine, N. D. Rago, J. Guo, T. Rojas, A. T. Ngo, K. Amine, *Nano Energy* **2022**, *92*, 106720.
- [57] K. Xu, *Chem. Rev.* **2004**, *104*, 4303.
- [58] J. B. Goodenough, Y. Kim, *Chem. Mater.* **2010**, *22*, 587.
- [59] K. Xu, S. S. Zhang, U. Lee, J. L. Allen, T. R. Jow, *J. Power Sources* **2005**, *146*, 79.
- [60] G.-X. Li, H. Jiang, R. Kou, D. Wang, A. Nguyen, M. Liao, P. Shi, A. Silver, D. Wang, *ACS Energy Lett.* **2022**, *7*, 2282.
- [61] L. Yu, S. Chen, H. Lee, L. Zhang, M. H. Engelhard, Q. Li, S. Jiao, J. Liu, W. Xu, J.-G. Zhang, *ACS Energy Lett.* **2018**, *3*, 2059.
- [62] A. Abouimrane, J. Ding, I. J. Davidson, *J. Power Sources* **2009**, *189*, 693.
- [63] Y. Yamada, C. H. Chiang, K. Sodeyama, J. Wang, Y. Tateyama, A. Yamada, *ChemElectroChem* **2015**, *2*, 1687.
- [64] Y. Wu, D. Ren, X. Liu, G. L. Xu, X. Feng, Y. Zheng, Y. Li, M. Yang, Y. Peng, X. Han, L. Wang, Z. Chen, Y. Ren, L. Lu, X. He, J. Chen, K. Amine, M. Ouyang, *Adv. Energy Mater.* **2021**, *11*, 2102299.
- [65] G. Yang, Y. Li, S. Liu, S. Zhang, Z. Wang, L. Chen, *Energy Storage Mater.* **2019**, *23*, 350.
- [66] T. Ma, G. L. Xu, Y. Li, L. Wang, X. He, J. Zheng, J. Liu, M. H. Engelhard, P. Zapol, L. A. Curtiss, J. Jorne, K. Amine, Z. Chen, *J. Phys. Chem. Lett.* **2017**, *8*, 1072.
- [67] E. Yoon, J. Lee, S. Byun, D. Kim, T. Yoon, *Adv. Funct. Mater.* **2022**, *32*, 2200026.
- [68] S. Lin, H. Hua, P. Lai, J. Zhao, *Adv. Energy Mater.* **2021**, *11*, 2101775.
- [69] H. Cheng, Q. Sun, L. Li, Y. Zou, Y. Wang, T. Cai, F. Zhao, G. Liu, Z. Ma, W. Wahyudi, Q. Li, J. Ming, *ACS Energy Lett.* **2022**, *7*, 490.
- [70] T. Hou, G. Yang, N. N. Rajput, J. Self, S.-W. Park, J. Nanda, K. A. Persson, *Nano Energy* **2019**, *64*, 103881.
- [71] H. Wang, S. C. Kim, T. Rojas, Y. Zhu, Y. Li, L. Ma, K. Xu, A. T. Ngo, Y. Cui, *J. Am. Chem. Soc.* **2021**, *143*, 2264.
- [72] J. Cao, D. Zhang, X. Zhang, Z. Zeng, J. Qin, Y. Huang, *Energy Environ. Sci.* **2022**, *15*, 499.
- [73] N. Yao, X. Chen, X. Shen, R. Zhang, Z. H. Fu, X. X. Ma, X. Q. Zhang, B. Q. Li, Q. Zhang, *Angew. Chem., Int. Ed.* **2021**, *60*, 21473.
- [74] Z. Piao, P. Xiao, R. Luo, J. Ma, R. Gao, C. Li, J. Tan, K. Yu, G. Zhou, H.-M. Cheng, *Adv. Mater.* **2022**, *34*, 2108400.
- [75] P. Xiao, R. Luo, Z. Piao, C. Li, J. Wang, K. Yu, G. Zhou, H.-M. Cheng, *ACS Energy Lett.* **2021**, *6*, 3170.
- [76] Y. Xiao, R. Xu, L. Xu, J.-F. Ding, J.-Q. Huang, *Energy Mater.* **2021**, *1*, 100013.
- [77] Y. Zou, Z. Cao, J. Zhang, W. Wahyudi, Y. Wu, G. Liu, Q. Li, H. Cheng, D. Zhang, G. T. Park, L. Cavallo, T. D. Anthopoulos, L. Wang, Y. K. Sun, J. Ming, *Adv. Mater.* **2021**, *33*, 2102964.
- [78] D. J. Yoo, S. Yang, K. J. Kim, J. W. Choi, *Angew. Chem., Int. Ed.* **2020**, *59*, 14869.
- [79] B. Horstmann, J. Shi, R. Amine, M. Werres, X. He, H. Jia, F. Hausen, I. Cekic-Laskovic, S. Wiemers-Meyer, J. Lopez, D. Galvez-Aranda, F. Baakes, D. Bresser, C.-C. Su, Y. Xu, W. Xu, P. Jakes, R.-A. Eichel, E. Figgemeier, U. Krewer, J. M. Seminario, P. B. Balbuena, C. Wang, S. Passerini, Y. Shao-Horn, M. Winter, K. Amine, R. Kostecki, A. Latz, *Energy Environ. Sci.* **2021**, *14*, 5289.
- [80] S. Ye, L. Wang, F. Liu, P. Shi, H. Wang, X. Wu, Y. Yu, *Adv. Energy Mater.* **2020**, *10*, 2002647.
- [81] Z. Liu, Y. Qi, Y. Lin, L. Chen, P. Lu, L. Chen, *J. Electrochem. Soc.* **2016**, *163*, A592.
- [82] Q. Zhang, J. Pan, P. Lu, Z. Liu, M. W. Verbrugge, B. W. Sheldon, Y.-T. Cheng, Y. Qi, X. Xiao, *Nano Lett.* **2016**, *16*, 2011.
- [83] K. Leung, *J. Phys. Chem. C* **2013**, *117*, 1539.
- [84] W. Liu, J. Li, W. Li, H. Xu, C. Zhang, X. Qiu, *Nat. Commun.* **2020**, *11*, 3629.
- [85] F. Li, J. He, J. Liu, M. Wu, Y. Hou, H. Wang, S. Qi, Q. Liu, J. Hu, J. Ma, *Angew. Chem., Int. Ed.* **2021**, *60*, 6600.
- [86] X. Cao, X. Ren, L. Zou, M. H. Engelhard, W. Huang, H. Wang, B. E. Matthews, H. Lee, C. Niu, B. W. Arey, Y. Cui, C. Wang, J. Xiao, J. Liu, W. Xu, J.-G. Zhang, *Nat. Energy* **2019**, *4*, 796.
- [87] M. He, R. Guo, G. M. Hobold, H. Gao, B. M. Gallant, *Proc. Natl. Acad. Sci. U. S. A.* **2020**, *117*, 73.
- [88] W. Huang, H. Wang, D. T. Boyle, Y. Li, Y. Cui, *ACS Energy Lett.* **2020**, *5*, 1128.
- [89] T. Kawamura, S. Okada, J.-i. Yamaki, *J. Power Sources* **2006**, *156*, 547.
- [90] A. Guéguen, D. Streich, M. He, M. Mendez, F. F. Chesneau, P. Novák, E. J. Berg, *J. Electrochem. Soc.* **2016**, *163*, A1095.
- [91] P. Biswal, J. Rodrigues, A. Kludze, Y. Deng, Q. Zhao, J. Yin, L. A. Archer, *Cell Rep. Phys. Sci.* **2022**, *3*, 100948.
- [92] S. Chen, J. Zheng, L. Yu, X. Ren, M. H. Engelhard, C. Niu, H. Lee, W. Xu, J. Xiao, J. Liu, J.-G. Zhang, *Joule* **2018**, *2*, 1548.
- [93] Y. Zhang, Y. Wu, H. Li, J. Chen, D. Lei, C. Wang, *Nat. Commun.* **2022**, *13*, 1297.
- [94] M. Mao, B. Huang, Q. Li, C. Wang, Y.-B. He, F. Kang, *Nano Energy* **2020**, *78*, 105282.
- [95] D. Aurbach, B. Markovsky, M. D. Levi, E. Levi, A. Schechter, M. Moshkovich, Y. Cohen, *J. Power Sources* **1999**, *81*, 95.
- [96] S. S. Zhang, *Electrochim. Commun.* **2006**, *8*, 1423.
- [97] H.-H. Sun, A. Dolocan, J. A. Weeks, R. Rodriguez, A. Heller, C. B. Mullins, *J. Mater. Chem. A* **2019**, *7*, 17782.
- [98] S. Jurng, Z. L. Brown, J. Kim, B. L. Lucht, *Energy Environ. Sci.* **2018**, *11*, 2600.
- [99] A. Fu, J. Lin, Z. Zhang, C. Xu, Y. Zou, C. Liu, P. Yan, D.-Y. Wu, Y. Yang, J. Zheng, *ACS Energy Lett.* **2022**, *7*, 1364.
- [100] X. Li, J. Liu, J. He, H. Wang, S. Qi, D. Wu, J. Huang, F. Li, W. Hu, J. Ma, *Adv. Funct. Mater.* **2021**, *31*, 2104395.
- [101] P. Zhou, Y. Xia, W. H. Hou, S. Yan, H. Y. Zhou, W. Zhang, Y. Lu, P. Wang, K. Liu, *Nano Lett.* **2022**, *22*, 5936.

- [102] Q. Liu, Z. Chen, Y. Liu, Y. Hong, W. Wang, J. Wang, B. Zhao, Y. Xu, J. Wang, X. Fan, L. Li, H. B. Wu, *Energy Storage Mater.* **2021**, *37*, 521.
- [103] K. Huang, S. Bi, B. Kurt, C. Xu, L. Wu, Z. Li, G. Feng, X. Zhang, *Angew. Chem., Int. Ed.* **2021**, *60*, 19232.
- [104] D. Wu, J. He, J. Liu, M. Wu, S. Qi, H. Wang, J. Huang, F. Li, D. Tang, J. Ma, *Adv. Energy Mater.* **2022**, *12*, 2200337.
- [105] S. Qi, J. He, J. Liu, H. Wang, M. Wu, F. Li, D. Wu, X. Li, J. Ma, *Adv. Funct. Mater.* **2020**, *31*, 2009013.
- [106] Z. Guo, X. Song, Q. Zhang, N. Zhan, Z. Hou, Q. Gao, Z. Liu, Z. Shen, Y. Zhao, *ACS Energy Lett.* **2022**, *7*, 569.
- [107] S. Zhang, G. Yang, Z. Liu, X. Li, X. Wang, R. Chen, F. Wu, Z. Wang, L. Chen, *Nano Lett.* **2021**, *21*, 3310.
- [108] X. Wang, S. Wang, H. Wang, W. Tu, Y. Zhao, S. Li, Q. Liu, J. Wu, Y. Fu, C. Han, F. Kang, B. Li, *Adv. Mater.* **2021**, *33*, 2007945.
- [109] X. Q. Zhang, X. Chen, X. B. Cheng, B. Q. Li, X. Shen, C. Yan, J. Q. Huang, Q. Zhang, *Angew. Chem., Int. Ed.* **2018**, *57*, 5301.
- [110] S. Gu, S. W. Zhang, J. Han, Y. Deng, C. Luo, G. Zhou, Y. He, G. Wei, F. Kang, W. Lv, Q. H. Yang, *Adv. Funct. Mater.* **2021**, *31*, 2102128.
- [111] C. Zhou, L. Zheng, T. He, M. A. Garakani, S. Abouali, Y. Shen, L. Chen, V. Thangadurai, *Energy Storage Mater.* **2021**, *42*, 295.
- [112] Q. Zhao, N. W. Utomo, A. L. Kocen, S. Jin, Y. Deng, V. X. Zhu, S. Moganty, G. W. Coates, L. A. Archer, *Angew. Chem., Int. Ed.* **2022**, *61*, 202116214.
- [113] H. Yang, X. Chen, N. Yao, N. Piao, Z. Wang, K. He, H.-M. Cheng, F. Li, *ACS Energy Lett.* **2021**, *6*, 1413.
- [114] X. Wang, S. Li, W. Zhang, D. Wang, Z. Shen, J. Zheng, H. L. Zhuang, Y. He, Y. Lu, *Nano Energy* **2021**, *89*, 106353.
- [115] Y. Wen, J. Ding, Y. Yang, X. Lan, J. Liu, R. Hu, M. Zhu, *Adv. Funct. Mater.* **2021**, *32*, 2109377.
- [116] Q. Liu, Y. Xu, J. Wang, B. Zhao, Z. Li, H. B. Wu, *Nano-Micro Lett.* **2020**, *12*, 176.
- [117] Y. Liu, D. Lin, Y. Li, G. Chen, A. Pei, O. Nix, Y. Li, Y. Cui, *Nat. Commun.* **2018**, *9*, 3656.
- [118] L. Fu, X. Wang, L. Wang, M. Wan, Y. Li, Z. Cai, Y. Tan, G. Li, R. Zhan, Z. W. Seh, Y. Sun, *Adv. Funct. Mater.* **2021**, *31*, 2010602.
- [119] X. Fan, L. Chen, X. Ji, T. Deng, S. Hou, J. Chen, J. Zheng, F. Wang, J. Jiang, K. Xu, C. Wang, *Chem* **2018**, *4*, 174.
- [120] Q. Liu, H. Xu, F. Wu, D. Mu, L. Shi, L. Wang, J. Bi, B. Wu, *ACS Appl. Energy Mater.* **2019**, *2*, 8878.
- [121] S. Chen, J. Zheng, D. Mei, K. S. Han, M. H. Engelhard, W. Zhao, W. Xu, J. Liu, J. G. Zhang, *Adv. Mater.* **2018**, *30*, 1706102.
- [122] N. Piao, X. Ji, H. Xu, X. Fan, L. Chen, S. Liu, M. N. Garaga, S. G. Greenbaum, L. Wang, C. Wang, X. He, *Adv. Energy Mater.* **2020**, *10*, 1903568.
- [123] S. C. Kim, X. Kong, R. A. Vila, W. Huang, Y. Chen, D. T. Boyle, Z. Yu, H. Wang, Z. Bao, J. Qin, Y. Cui, *J. Am. Chem. Soc.* **2021**, *143*, 10301.
- [124] X. Fan, X. Ji, L. Chen, J. Chen, T. Deng, F. Han, J. Yue, N. Piao, R. Wang, X. Zhou, X. Xiao, L. Chen, C. Wang, *Nat. Energy* **2019**, *4*, 882.
- [125] D.-J. Yoo, S. Yang, Y. S. Yun, J. H. Choi, D. Yoo, K. J. Kim, J. W. Choi, *Adv. Energy Mater.* **2018**, *8*, 1802365.
- [126] W. Zhang, Y. Guo, T. Yang, Y. Wang, X. Kong, X. Liao, Y. Zhao, *Energy Storage Mater.* **2022**, *51*, 317.
- [127] W. Li, A. Dolocan, J. Li, Q. Xie, A. Manthiram, *Adv. Energy Mater.* **2019**, *9*, 1901152.
- [128] Y. X. Yao, X. Chen, C. Yan, X. Q. Zhang, W. L. Cai, J. Q. Huang, Q. Zhang, *Angew. Chem., Int. Ed.* **2021**, *60*, 4090.
- [129] C.-C. Su, M. He, R. Amine, Z. Chen, R. Sahore, N. D. Rago, K. Amine, *Energy Storage Mater.* **2019**, *17*, 284.
- [130] J. Holoubek, M. Yu, S. Yu, M. Li, Z. Wu, D. Xia, P. Bhaladhare, M. S. Gonzalez, T. A. Pascal, P. Liu, Z. Chen, *ACS Energy Lett.* **2020**, *5*, 1438.
- [131] P. Xiao, Y. Zhao, Z. Piao, B. Li, G. Zhou, H.-M. Cheng, *Energy Environ. Sci.* **2022**, *15*, 2435.



Zhihong Piao received her bachelor's degree from the School of Materials Science and Engineering, Tsinghua University in 2020. She is now a Ph.D. student at Tsinghua Shenzhen International Graduate School, Tsinghua University under the supervision of Prof. Hui-Ming Cheng and Prof. Guangmin Zhou. Her research interest focuses on the design of electrolyte and interface for high-energy-density battery systems.



Runhua Gao gained his bachelor's degree from Fudan University in 2020 and he is now pursuing his Ph.D. degree in Tsinghua University under the supervision of Prof. Guangmin Zhou. His research interest focuses on the development of flexible and high energy density rechargeable batteries.



Yingqi Liu received her BS degree (2019) from the School of Materials Science and Engineering, Northeastern University. Now, she is a Ph.D. student of Tsinghua-Berkeley Shenzhen Institute, Tsinghua University. Her research interests focus on developing bidirectional catalysts for reversible Li–CO₂ batteries.



Guangmin Zhou is an associate professor in Tsinghua Shenzhen International Graduate School, Tsinghua University. He received his Ph.D. degree from Institute of Metal Research, Chinese Academy of Sciences in 2014 under the supervision of Prof. Hui-Ming Cheng and Prof. Feng Li, and then worked as a postdoc in UT Austin with Prof. Arumugam Manthiram during 2014–2015. After that, he was a postdoc fellow in the Department of Materials Science and Engineering at Stanford University with Prof. Yi Cui from 2015 to 2019. His research mainly focuses on the development of advanced energy-storage materials and devices and battery recycling.



Hui-Ming Cheng is a professor of Institute of Technology for Carbon Neutrality, Shenzhen Institute of Advanced Technology, Chinese Academy of Sciences, and the Advanced Carbon Research Division at Shenyang National Laboratory for Materials Science, Institute of Metal Research, Chinese Academy of Sciences, and the Low-Dimensional Material and Device Laboratory of the Tsinghua-Berkeley Shenzhen Institute, Tsinghua University. His research activities focus on carbon nanotubes, graphene, 2D materials, energy storage materials, photocatalytic semiconducting materials, and bulk carbon materials.